Chapter 6
Materials for Tribology

Different engineering parts are subjected to tribological loading, such as sliding at different loads and speeds, abrasive interactions with hard particles or repeated contact stresses. Therefore, it is necessary to select materials according to specific engineering requirements, and then to verify their ability to perform adequately under the acting wear conditions. In this respect, for applications with demanding tribological loadings, materials with specially designed tribological properties have been developed.

In the previous chapter, indications for the use of materials that better resist different wear processes were given. This chapter provides a more detailed overview of the engineering materials that are more frequently employed in tribological applications. For each class of materials, an outline of the relevant behaviour with respect to sliding wear, characterized by the mechanisms of adhesive and tribo-oxidative wear, wear by contact fatigue, and abrasive wear by hard granular material, will be provided. Specific surface treatments may be also adopted to improve the tribological properties of materials; they will be considered in the next chapter.

6.1 Steels

Steels are widely used in tribological applications, in like-on-like couplings or in combination with other materials. Particular steel grades have been developed for specific applications. Some examples are:

(1) tool steels;
(2) bearing steels;
(3) Hadfield steels (austenitic steels with high abrasion resistance);
(4) martensitic stainless steels for applications in aggressive environments.

By varying the chemical composition and/or by appropriate heat treatments (including surface treatments), it is possible to obtain steels with a wide a range of

G. Straffelini, *Friction and Wear*, Springer Tracts in Mechanical Engineering,
DOI 10.1007/978-3-319-05894-8_6

Table 6.1 Surface phenomena that can occur at a steel surface during tribological interaction (modified from [2])

Phenomenon	Type of steel	Strain induced	Temperature induced
(1) Stress relieving	All	–	X
(2) Recristallization	All	X	X
(3) Tempering	Martensitic	–	X
(4) Strain hardening	All	X	–
(5) Strain-induced martensitic transformation	• Hadfield steel • Some austenitic stainless steels • Martensitic steels containing retained austenite	X	–
(6) Thermal martensitic transformation	Quench hardenable steels	–	X
(7) Precipitation hardening	High alloy steels	–	X
(8) Oxidation	All	–	X
(9) Melting	All	–	X

properties, as concerns mechanical strength and fracture toughness [1, 2]. In particular, hardness values up to 800–1000 kg/mm^2 can be attained.

During the tribological interactions, plastic deformations and energy dissipation with related temperature rise usually take place at the contacting asperities. In steels, both phenomena may produce local microstructural changes that are very important from the viewpoint of tribology. They are summarized in Table 6.1. The phenomena numbered from 1 to 3 all cause a reduction in hardness at the contacting asperities, while a material hardening is induced by the phenomena from 4 to 7. Oxidation (no. 8 in the table) induces the formation of a surface oxide layer, which, under particular conditions, may decrease friction and wear. Melting (no. 9 in the table) may only occur under particularly severe sliding conditions.

6.1.1 Sliding Wear

In case of mild wear steels display specific wear coefficients (K_a) typically ranging from 10^{-15} to 10^{-14} m^2/N. For adhesive wear, K_a takes much higher values, typically around 10^{-12} m^2/N. The iron oxides have a hardness in the range 300–600 kg/mm^2 that strongly decreases as temperature is increased [3]. Therefore, the use of a steel with high hardness is very important. In fact, a suitably hard steel would be particularly capable to support the oxide layer and, in addition, not to be abraded by the oxide fragments during sliding. This is well shown in Fig. 6.1a, for a C60 steel (a non-alloy steel containing 0.6 % C) after different thermal treatments, like: normalizing, to obtain a hardness of 200 kg/mm^2; quenching and tempering to

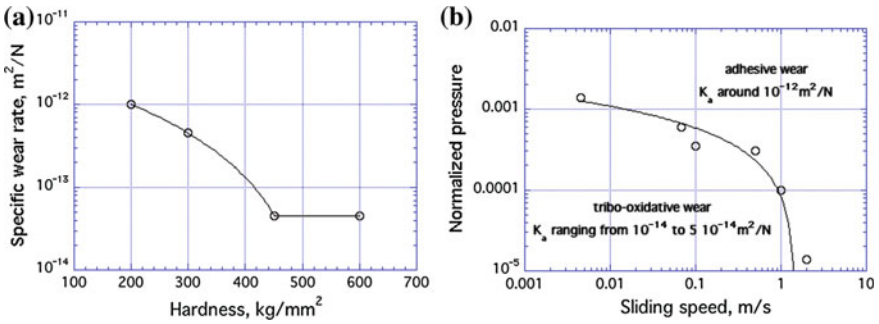

Fig. 6.1 **a** Specific wear rate as a function of hardness for a C60 steel, subject to dry sliding with $p_0 = 1.3$ MPa and v = 0.1 m/s. The steel hardness was changed by adopting suitable heat treatments (modified from [4]). **b** Wear map for steels, in case of relatively low sliding speeds and applied pressures (from different literature references)

obtain a hardness of 300 and 450 kg/mm^2; and quenching and stress relief to obtain a hardness of 600 kg/mm^2. When hardness exceeds 450 kg/mm^2 wear is mainly by tribo-oxidation and the corresponding K_a-values are typical of mild wear. It is worth recalling that this process is fully effective when fragments are allowed to remain in the contact region.

In order to be able to compare the behaviour of materials with different hardness values, the concept of *normalized pressure* has been introduced. It is defined as the ratio between the nominal pressure and the materials' hardness (that of the softer one, if the mating materials are different):

$$\bar{p} = \frac{F_N}{A_n H} = \frac{p_0}{H} \tag{6.1}$$

For example, the data in Fig. 6.1a show that at v = 0.1 m/s the transition between adhesive and tribo-oxidative wear occurs for hardness values between 400 and 450 kg/mm^2, i.e., for a normalized pressure about 3×10^{-4}. Using this information and additional data taken from the literature (referring to pin-on-disc tests with the fragments able to remain in the contact region), it is possible to construct the wear map shown in Fig. 6.1b. It can be observed that at low sliding speeds, typically lower than 0.1 m/s, the boundary between tribo-oxidative (mild) wear and adhesive (severe) wear is mainly dependent on the normalized pressure. In fact, it is determined by the ability of the steel (in relation to the applied pressure) to support the layer of protective oxides forming on its surface. For sliding speeds in excess of 0.1 m/s, the frictional heating gains in importance and the boundary between tribo-oxidative and adhesive wear is controlled both by normalized pressure and sliding speed, i.e., by the attainment of a critical surface temperature, at which softening is so intense to prevent the steel substrate to properly sustain the surface oxide layer (item 1 in Table 6.1).

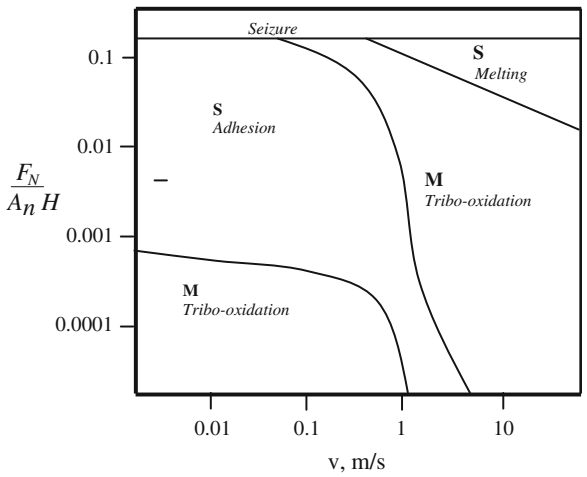

Fig. 6.2 Scheme of wear map for steels (*M* mild wear; *S* severe wear)

Using the data collected by Lim and Ashby [5], it is possible to construct a complete wear map for steels under dry sliding. It is schematically shown in Fig. 6.2. It may be noted that for high normalized pressures (greater than about 0.2), *seizure* occurs regardless of the sliding speed. Under these conditions, the actual area of contact approaches the nominal one, and wear (by adhesion) becomes extremely severe, with intense material transfer. A new region is introduced at high sliding speeds and high normalized pressures, i.e., *melting wear*. In this region, frictional heating is so high to induce melting of the asperities, and wear is consequently severe. At high sliding speeds (greater than 1 m/s) and lower normalized pressure, melting cannot occur and (mild) tribo-oxidative wear by direct oxidation occurs (Sect. 4.2.1). If the sliding speed is between 1 and 10 m/s, martensite can form in the contact regions during sliding (item 5 in Table 6.1). Such a formation is a consequence of the attainment of high flash temperatures that induce local austenitization, and by the following rapid cooling caused by the intense heat removal exerted by the bulk material. Such a martensite layer (which is sometimes called *white layer* because of its appearance after metallographic etching), helps supporting the surface oxide layer, counteracting the thermal softening. For particularly high speeds (v > 10 m/s), the oxide layer becomes very thick and it plastically spreads onto the contact surface, thereby contributing to an efficient dissipation of heat and thus preventing the attainment of high average surface temperatures.

To ensure the best performance in dry sliding, steels should then possess high hardness and they should also be able to maintain a relatively high hardness even with increasing contact temperature. The best candidates for dry sliding applications are therefore:

- nitrided steels;
- tool steels;
- carburized steels;

Table 6.2 Chemical compositions and typical mechanical properties of some tool steels

Type of steel	Hardness (kg/mm^2)	Charpy-V impact energy (J)	Material (AISI code)	Typical chemical composition					
				% C	% Mn	% W	% Cr	% Mo	Other
Cold work tool steel	650–850	3	O1	0.9	1	0.5	0.5	–	–
			D2	1.5	0.3	–	12	1	1 % V
Hot work tool steel	400–700	15	H11	0.35	–	–	5	1.5	1 % Si, 0.4 % V
			H13	0.35	–	–	5	1.5	1 % V
High-speed steel	800–1000	8	T15	1.5	–	12	4	–	5 % V
									5 % Co
			M2	0.8	–	6	4	5	2 % V

- heat treated (martensitic) steels;
- bearing steels.

Nitrided and carburized steels will be described in the next chapter. Here the attention will be firstly focussed on *tool steels*, which have been specially developed for the production of processing tools, such as dies and moulds, that are intensively subjected to sliding wear (mainly under dry or boundary lubricated conditions). Tool steels are classified into three groups: *cold work* steels, *hot work* steels, and *high-speed* steels. Table 6.2 shows the chemical compositions, typical hardness and impact fracture energy values of some common tool steels (after quenching and tempering). The steels are indicated according to the AISI (American Iron and Steel Institute) code.

After machining and heat treatment, tool steels will generally have a microstructure comprising a martensitic matrix and a carbide dispersion of the added elements. As an example, Fig. 6.3 shows the microstructure of two widely used steels, AISI D2 and AISI M2. Cold work tool steels (series W, A, O, and D) have a

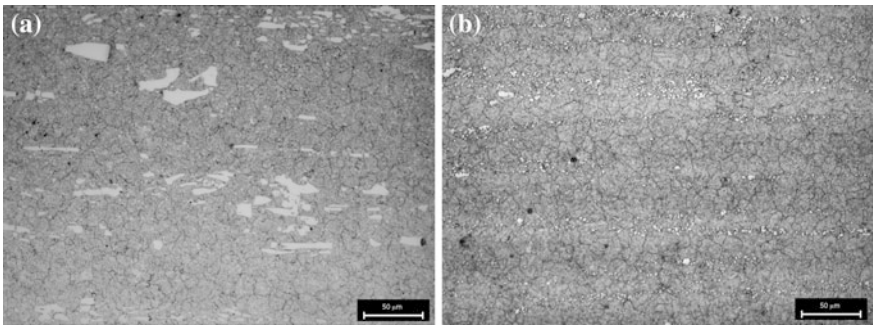

Fig. 6.3 Microstructures of the AISI D2 (**a**) and AISI M2 (**b**) tool steels. Note the presence of quite large primary carbides in AISI D2

high carbon content (>1 %), and contain other alloying elements such as chromium, tungsten and manganese. Chromium, which is particularly present in steels of D series, and tungsten form relatively large primary carbides (typically around 10 μm in size), while manganese is added to increase matrix hardenability. These steels are fairly cheap and have a maximum operating temperature of 200–300 °C. Hot work tool steels have a low carbon content and correspondingly display a high fracture toughness. If tempered at about 600 °C after quenching, they acquire a high hardness, due to the precipitation of fine carbides (*secondary hardening*). Because of this, they are able to maintain a high hardness up to temperatures of about 540 °C. Finally, high-speed steels feature a high carbon content, and other alloying elements such as tungsten, chromium and vanadium. They are characterized by high hardness, retained even at high temperatures, as they also display a secondary hardening. Fracture toughness of high-speed steels is clearly lower than that of hot work tool steels. Some high-speed steels also contain cobalt, which provides an increased hardness at high temperatures.

In order to obtain mild tribo-oxidative wear in dry sliding, it is suggested to use steels containing small and uniformly dispersed carbides, to avoid any possible abrasive action from the largest carbides. This is also important in case of sliding under boundary lubrication conditions.

Figure 6.4 schematically shows the dependence of hardness on the environmental temperature, in the case of hot work tool steels and high-speed steels. Note that even the AISI D2 cold work tool steel is able to maintain a hardness of about 400 kg/mm^2 up to 600 °C, if it has been previously quenched and tempered to a hardness of about 700 kg/mm^2.

Heat-treated martensitic steels may achieve quite high hardness values (typically up to 800 kg/mm^2), depending on carbon content, alloying elements and heat-treatment cycle. Steels with a high amount of alloy elements may contain some *retained austenite* (RA) in their microstructure after the heat treatment. The role of RA on the sliding resistance of steels (as well as on their contact fatigue behaviour) has not yet completely clarified. It is believed that if RA is unstable (i.e., it contains

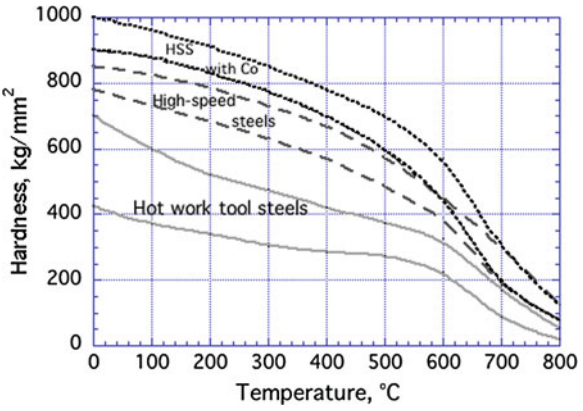

Fig. 6.4 Hardness versus temperature for hot work tool steels and high-speed tool steels

a small amount of alloying elements) and can then easily transform into martensite by surface shear deformation, its role is positive in that it induces a local strength increase (the amount of RA, however, has to be controlled to avoid excessive distortions associated with the austenite to martensite transformation). If RA is stable, however, it does not harden during sliding, and it may become a weak microstructural region, where an intense plastic deformation can concentrate.

In applications where high fracture toughness and ductility are required, or when thermal treatment is difficult to be performed, martensitic steels are not suitable, and *pearlitic steels* may be preferable. Due to the intense surface plastic deformation during sliding, the cementite lamellae of these steels are oriented in the direction of sliding, significantly increasing the mechanical strength and thus the wear resistance. Typical pearlitic steels contain 0.7 % carbon and 1.5 % manganese that reduces the pearlite interlamellar spacing. Pearlitic steels with a hardness between 300 and 350 kg/mm^2, display a sliding wear resistance that is comparable to that of bainitic and martensitic steels [6].

6.1.2 Wear by Contact Fatigue

The steels that guarantee the best resistance against contact fatigue are the so-called *bearing steels*, which are specially developed to produce the rolling elements and raceways of bearings. These steels are characterized by high hardness, excellent dimensional stability in service, and high degree of homogeneity and microstructural quality. These steels are produced with a very low content of inclusions, such as oxides, sulphides and nitrides, and a high surface finish. As said, the reduction in concentration and dimension of the inclusions decreases the probability that an inclusion of a critical size is found in the most stressed area, i.e., close to the distance z_m from the surface (Table 1.1). Steels with extreme cleanliness are now produced using special secondary metallurgical technologies, such as vacuum induction melting (VIM) and vacuum arc remelting (VAR).

The most common bearing steel is the *AISI 52100* (also indicated with 100Cr6), which contains 1 % carbon and 1.45 % chromium [7]. This steel is quenched and tempered at about 160 °C to ensure the obtainment of high hardness, typically between 650 and 1000 kg/mm^2. To increase its dimensional stability, the steel is often subjected to a soaking at −80 °C before tempering, aiming at completely eliminate residual austenite present after quenching (usually about 6 %). It is clear that the in-service temperature should not exceed 200 °C to avoid microstructural softening. In order to obtain higher surface hardness values, and thus higher contact fatigue resistance, specific steels may be exposed to a *carburizing* (or carbonitriding) treatment, obtaining a graded microstructure with a carbon enrichment at the surface and consequent introduction of compressive residual stresses. The M50 NiL steel (typically containing 0.13 % C, 3.5 % Ni, 4 % Cr, 4.25 % Mo, 1.2 % V) is commonly used in the carburized state, with a surface hardness of about 750 kg/mm^2 and a hardness greater than 550 kg/mm^2 for a depth of at least 1.5 mm [8].

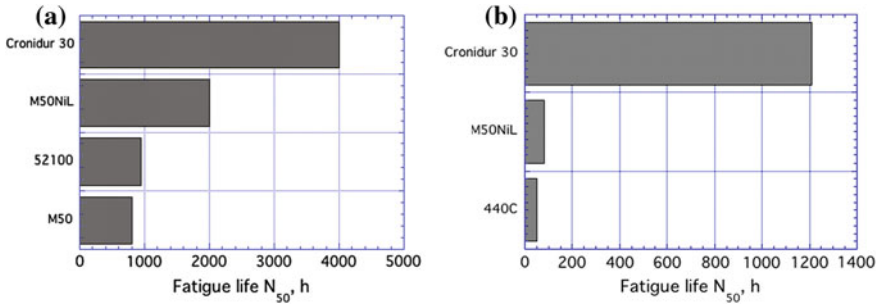

Fig. 6.5 Contact fatigue life of different high strength steels tested in (**a**) fluid film lubrication, and in (**b**) boundary lubrication. The Hertzian pressure was 2800 MPa and the oil temperature was maintained at 90 °C (**a**) and 95 °C (**b**) (modified from [9])

Surface treated steels retain a good fracture toughness in the bulk and are thus very suitable for engineering applications that require both high contact fatigue resistance and high fracture toughness. In some applications, such as in advanced aerospace engines, wind turbines and high-speed railways, a further increase in hardness and fatigue strength may be required. It can be achieved by using *high nitrogen martensitic steels*, where the sum of the carbon and nitrogen content is tuned between 0.6 and 0.8 %. Figure 6.5 shows the results of bearing life tests carried out on several high-strength steels with a rather high contact fatigue resistance (Cronidur 30, X30CrMoN15-1, containing 0.38 % N, 15 % Cr and 1 % Mo; it is used in the martensitic state) [9].

In case of ambient temperatures exceeding 200 °C, other types of steels are required, such as the M series of the high-speed steels (e.g., AISI M2) that display the secondary hardening phenomenon. In the presence of corrosive environments (commonly encountered, for example, in aircraft engines and in the paper industry), martensitic stainless steel containing at least 17 % chromium are employed. An example is the AISI 440C, with nominal chemical composition: 1 % C, 0.4 % Mn, 0.3 % Si, 17 % Cr, 0.5 % Mo. With a suitable heat treatment, it can reach a hardness level similar to that of tool steels. Because of the presence of carbon, however, this steel also contains large eutectic carbides in its microstructure, which may reduce corrosion resistance and also fatigue strength. For these reasons, steels with lower chromium content may be used instead. When using the abovementioned high nitrogen martensitic steels (containing 13 % Cr approx.), the formation of large eutectic carbides is avoided and the corrosion resistance, in specific environments, in maintained [7].

6.1.3 Abrasive Wear by Hard, Granular Material

According to what reported in Sect. 5.4, the steels with the best abrasive wear resistance are those with a microstructure constituted by high carbon martensite and

hard and large carbides. It should be noted that martensitic steels (without large carbides) can reach maximum hardness values of about 1000 kg/mm^2, inadequate for many abrasive particles, including silica particles that are the most common natural abrasives. The presence of large and hard carbides in the microstructure is then paramount for steels to gain an excellent resistance to abrasive wear (see, for example, the behaviour of the AISI D2 tool steel in Fig. 5.19a).

Steels are commonly used in applications where abrasive wear is present, because they can retain some ductility even when they possess high hardness, and also because of their relatively low cost. The most commonly used steels are, in descending order [10]:

(1) Cold work tool steels and high-speed steels, containing 1–1.6 % C (hardness about 800–900 kg/mm^2);
(2) Hot work tool steels, containing about 1 % C (hardness about 600–900 kg/mm^2);
(3) Martensitic steels, containing about 0.7 % C and possibly other alloying elements to increase their hardenability (hardness about 600 kg/mm^2);
(4) Pearlitic Cr-Mo steels containing 1 % C (hardness about 350 kg/mm^2 only, but greater ductility than tool steels);
(5) Austenitic manganese steels, like the *Hadfield steels* containing 12–14 % Mn and 1 % C. These steels have initial hardness values around 200 kg/mm^2, but due to the strain-induced martensitic transformation (item 5 in Table 6.1) they achieve hardness values in the range 400–500 kg/mm^2 in the contact region.

The *austenitic manganese steels*, such as the Hadfield steels, are used if high fracture toughness is required, for example when the mechanical parts have to stand impact loads. These steels are therefore mainly used in applications characterized by high-stress abrasion wear. Since they are quite difficult to machine by chip removal (due to the hardening effect during cutting), they are mainly used in the as-cast state, or as deposited surface layers. Manganese steels harden during plastic deformation because of the shear-induced transformation of austenite into martensite. If such a transformation can take place during the tribological interaction, the abrasion resistance of these materials increases dramatically. The martensitic transformation is favoured if the austenite is unstable, that is, if relatively low concentrations of carbon and manganese are present [11]. It should be noted that manganese steels contain a certain amount of carbides (iron and chromium carbides) in their microstructure after solidification. Therefore, they should be submitted to a solution treatment at about 1050 °C before being placed in service in order to obtain a fully austenitic microstructure.

Figure 6.6 summarizes, in a simplified way, the abrasive wear resistance of various ferrous alloys, including white irons that will be discussed in the next section.

In many applications, abrasion occurs in the presence of an aggressive environment. When the environment is very aggressive and the abrasive action is limited, austenitic stainless steels can be used: next to a very high corrosion resistance in specific environments, they can ensure a sufficient abrasion resistance

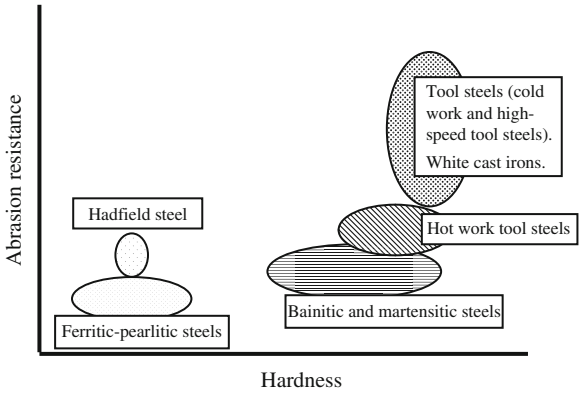

Fig. 6.6 Schematization showing the abrasion resistance of different ferrous alloys (modified from [12])

exploiting their ability to work harden during deformation (see Fig. 5.19a). In other applications, however, higher hardness may be required, and the martensitic stainless steels, such as AISI 440, should be employed.

6.2 Cast Iron

Cast irons are Fe–C alloys with a carbon content between 2 and 4 % and a silicon content between 1 and 3 %. They are very suitable for the production of castings and are then commonly used for manufacturing particular mechanical components (including large parts or components with very complex shapes). High levels of silicon allow carbon to solidify in the form of graphite. On the other hand, if silicon content is relatively low and the cooling rate, during solidification, is high, carbon forms carbides, whose composition depend on the alloying elements. Table 6.3

Table 6.3 Main characteristics of cast irons

Cast iron	Hardness	% C	Microstructure	Observations
Grey	Moderate (≈200 kg/mm^2)	<3	Lamellar graphite; matrix: F, P, B, M	Most common iron
Ductile (or nodular)	Moderate (≈350 kg/mm^2)	2.5–4	Spheroidal graphite; matrix: F, P, B, M, AF	High fatigue resistance; complex shapes
White	High (420–600 kg/mm^2)	4.2–5.6	Large eutectic and secondary carbides	Alloying elements can be profitably added (Ni, Cr)
			Matrix: M, B	
Malleable	Moderate (≈250 kg/mm^2)	≈2.5	"Flowerlike" nodular graphite	Properties similar to steels
			Matrix: F, P	

F ferrite, *P* pearlite, *B* bainite, *M* martensite, *AF* ausferrite; modified from [1]

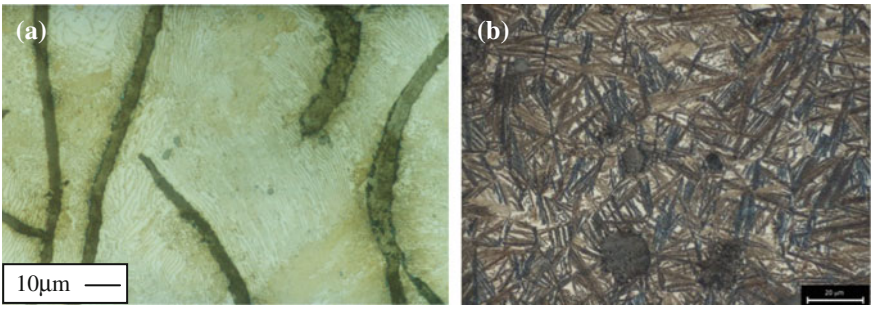

Fig. 6.7 Microstructure of **a** a pearlitic grey iron, and **b** an ADI characterized by a graphite fraction of 7.2 %, an average nodule count of 195, a mean nodule diameter of 15 μm, and an amount of retained austenite of 25 % [14]

summarizes the main types of cast irons and relevant features. The matrix microstructure of graphitic cast irons is typically similar to that of steels. Within the family of ductile (or nodular) irons, *austempered ductile irons* (ADIs) have recently reached a widespread diffusion. They are obtained following an austempering treatment that usually comprises austenitisation between 850 and 950 °C, followed by quenching in a salt bath furnace at 250–400 °C. The material is then kept at this temperature for a time suitable to stabilize austenite, and then it is cooled down to room temperature. An *ausferritic* (AF) microstructure is obtained, characterized by the presence of bainitic ferrite plus carbon stabilized austenite, that increase strength and ductility [13]. As an example, Fig. 6.7 shows the microstructure of a pearlitic grey iron and an austempered ductile iron.

Cast irons are characterized by an attractive combination of mechanical properties and advantages, concerning cost and manufacturing. The high hardness that is obtainable with thermal treatments and the addition of alloying elements, allow cast irons to be used in several tribological applications. For example, if sliding wear problems are of concern, grey or ductile cast irons are widely used, in like-on-like applications or against steel or copper alloys (such as bronzes). In the case of abrasive wear processes, white cast irons are profitably used, indeed.

6.2.1 Sliding Wear

Grey and ductile cast irons are commonly employed in tribological systems characterized mainly by sliding wear, both in dry and in boundary lubricated conditions. Typical applications are disc brakes, piston rings, cylinder liners, cam-follower systems and gears. The applications relate mostly to situations where lubrication, particularly fluid film, is difficult to obtain, or, on the contrary, undesirable.

The high sliding wear resistance of grey or ductile iron is due to the presence of graphite, which acts as a solid lubricant during sliding. In fact, during the run-in

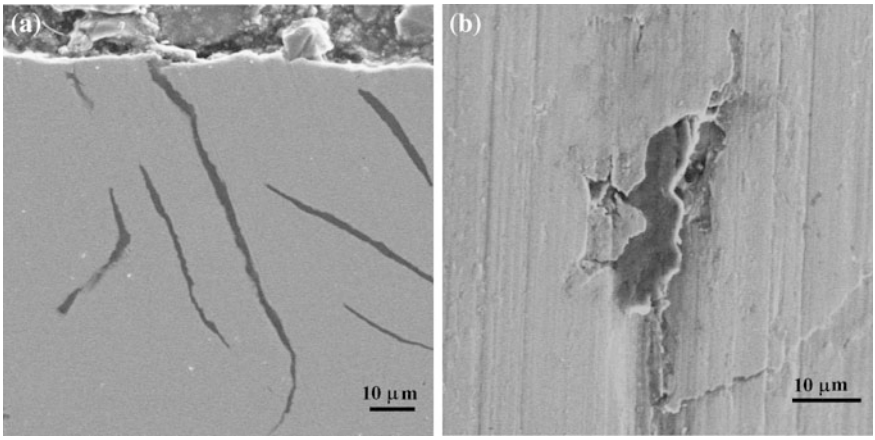

Fig. 6.8 **a** Cross section showing a graphitic lamella emerging at the surface during dry sliding; **b** graphite is rubbed on the wear surface thus exerting a solid lubricant effect [15]

phase graphite protrudes from the surface and is interposed between the two mating bodies. This is shown, for example, in Fig. 6.8, referring to a pearlitic grey cast iron after dry sliding against a friction material [15]. This phenomenon may thus work together with the formation of a surface oxide, which ensures the establishment of a mild tribo-oxidative wear. As a result, a reduction in friction and sliding wear are attained. As shown in Table 5.2, the pearlitic or martensitic grey cast irons are characterized by specific wear coefficients similar to those of tool steels, although their hardness values are significantly lower.

As observed in steels, a transition to severe adhesive wear may occur if the contact pressure increases above a critical value. Figure 6.9 shows the experimental dependence of the nominal pressure, at the transition from mild to severe wear, on the carbon content, i.e., on the fraction of graphite flakes, in the case of a pearlitic

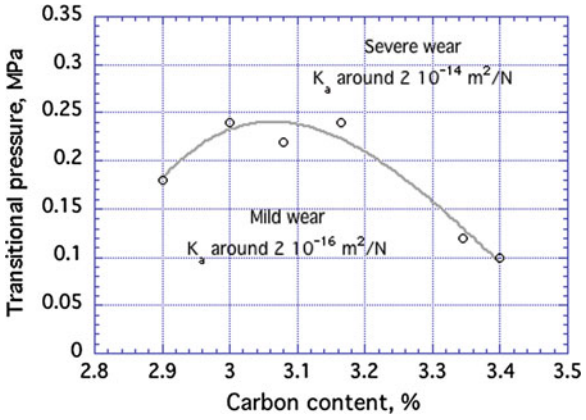

Fig. 6.9 Nominal contact pressure at the transition between mild and severe wear as a function of carbon content, in a pearlitic gray cast iron dry sliding against in high strength steel (modified from [16])

grey cast iron (with microhardness of the pearlite matrix around 440 kg/mm^2) [16]. It can be noted that the transition pressure displays a maximum at about 3.05 % C. This maximum is due to the fact that an increase in graphite content increases the solid lubricant effect and, at the same time, induces a decrease in the load-bearing area, i.e., in the fraction of metal that supports the contact stress. For a given grey cast iron, the transition pressure also decreases with increasing the sliding speed, as observed in steels and in other alloys, because of the thermal softening effect at the contact regions.

If the graphite is present in the form of nodules (or *spheroids*, ductile or nodular cast iron) instead of lamellae the sliding wear resistance is higher in the presence of relatively high nominal pressures. Indeed, while the lubricating effect of the graphite remains almost unchanged, the spheroids give rise to a lower stress concentration thus reducing the tendency to subsurface damage influencing adhesive wear. However, at relatively low loads the geometry of the lamellar graphite is preferable, since the feeding of the contact surface by graphite flakes is easier. In addition, lamellar graphite realizes a greater thermal conductivity than nodular graphite, inducing a better capacity of remove the frictional heat from the contact surface.

Regarding the influence of the matrix microstructure, it has to be observed that ferritic or austenitic matrices are generally to be avoided because they are too soft. Cast irons are then preferably to be used with pearlitic, martensitic or austempered matrix microstructures. In general, if ambient temperature is lower than 250 °C, ADI is superior to quenched and tempered ductile irons with comparable hardness values, because the strain-induced transformation of retained austenite and the strain hardening of bainitic ferrite contribute to the oxidation wear resistance by better supporting the surface oxide layer [17].

As mentioned before, grey and ductile irons are also satisfactory employed in the case of lubricated sliding under boundary conditions. In this respect, it has to be further observed that ductile iron with an austempered microstructure may display an higher scuffing resistance than heat-treated steels, since free graphite reduces friction and hence the temperature rises at the contacting asperities.

6.2.2 Wear by Contact Fatigue

Gray and ductile cast iron with a pearlitic or austempered microstructure are employed in many applications where contact fatigue damage may occur, such as in gears or cams. The main advantages are the possibility of obtaining near-net shapes with casting techniques, and also the high machinability by chip removal.

Grey cast irons display a resistance to contact fatigue that is only about 60 % that of the fatigue resistance of steels with the same hardness level. This reduction is due to the negative effect of the graphite lamellae, which exert a stress concentration at their edges, facilitating the nucleation of fatigue cracks. In addition, the lamellae also provide an energetically favourable path for crack propagation. Because of

this, grey cast irons are typically characterized by a value of the coefficient n in Eq. 5.8 that is definitely higher than that of steels. Ductile iron displays a better contact fatigue resistance, especially after austempering. The graphite nodules, in fact, facilitate the nucleation phase, although to a lower extent than the lamellae, but they do not provide any favourable path for the subsequent crack propagation. Indeed, when the propagating crack intersects graphite nodules it may be stopped or at least slowed down in its propagation rate. The contact fatigue endurance limit of ductile irons is therefore only 10–15 % lower than that of steels of the same hardness [18]. Thanks to their ausferritic microstructure, ADIs are characterized by a relatively high fracture toughness that makes them particularly attractive for the production of gears.

A way to improve further the contact fatigue resistance of nodular cast irons is to increase the density of graphite nodules, and, consequently, to reduce their average size. Typically the nodular cast irons contain a density of nodules between 200 and 250 nodules/mm^2. By increasing the cooling rate during solidification (and, simultaneously, using high levels of silicon which promotes graphitization), cast irons containing more than 1000 nodules/mm^2 can be obtained [19].

6.2.3 Abrasive Wear by Hard Particles

As mentioned, white cast irons possess high resistance to abrasive wear. In particular, *high-chromium white cast irons* with high content of primary carbides of the type $(Fe, Cr)_7C_3$ are widely used. These materials typically contain: 1.2–3.5 % C, 0.3–1.5 % Si, 0.4–1.5 % Mn, 15–32 % Cr, 0.5–3 % Mo, 1–3 % Cu and have hardness ranging from 850 to 900 kg/mm^2. The *nickel-chromium martensitic white cast irons* are also commonly used in practice. The addition of nickel, which does not form carbides, increases hardenability of the alloy, i.e., its attitude to form martensite even at relatively low cooling rates. These irons typically contain: 2.6–3.6 % C, 0.4–1 % Si, 0.4–0.8 % Mn, 1–2.5 % Cr, 3.5-5 % Ni and have hardness values between 560 and 700 kg/mm^2.

After solidification, white cast irons achieve a microstructure consisting of carbides in an austenitic matrix. Because of the high content of alloying elements austenite is stabilized at room temperature. These irons may be then used in the as-cast condition in applications with low-stress abrasive wear. In fact, during the abrasive interactions the austenite transforms into martensite, as already observed in the manganese steels. However, to get the best abrasive wear resistance, including the high-stress abrasion resistance, it is necessary to heat treat the alloys to obtain a fully martensitic matrix microstructure. Since austenite is stabilized by chromium, a soaking treatment is initially carried out at 900–1000 °C to promote the precipitation of chromium carbides thus destabilizing the austenite. Subsequently, the quenching and relieving treatment is performed to obtain the martensitic matrix.

Figure 6.10 shows a typical microstructure of a martensitic white cast iron. Note the presence of primary carbides that form a three-dimensional network giving rise

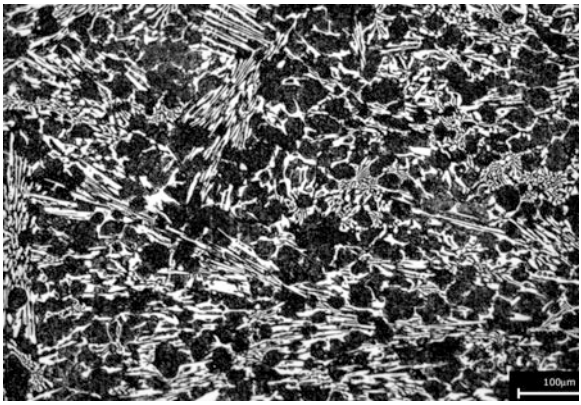

Fig. 6.10 Typical microstructure of a martensitic white cast iron

to high hardness but also noticeable brittleness. In many applications, as in the case of the cylinders for rolling mills, the solidification aims at obtaining a surface rim of white cast iron and a core of nodular (ductile) cast iron, able to provide the component an adequate fracture toughness (the process used is *centrifugal casting*).

The abrasive resistance of white cast irons depends on several factors, such as the type and volume fraction of the carbides, the matrix hardness, the hardness, size, and the angularity of the abrasive particles. As already remarked, chromium carbides have a hardness of about 1500–1800 kg/mm^2 and therefore may well resist the abrasive action of particles with lower hardness (such as silica or alumina). However, they do not offer adequate resistance in the case particles, such as those of SiC, with higher hardness (see also Fig. 5.19b). To increase the abrasive wear resistance of the white irons in the latter case, it is therefore necessary to introduce alloying elements, such as vanadium, capable of forming harder carbides (Table 2.1).

6.3 Copper Alloys

Copper alloys are used in several tribological applications characterized by sliding wear or wear by contact fatigue in mixed or boundary lubrication (such as in gears, bearings, seals, just to mention some important examples), especially when the counterface is made of steel and the environment is aggressive. Beside quite excellent tribological properties (except the abrasion resistance, which is very low), copper alloys are characterized by other attractive engineering properties, such as high thermal conductivity and high corrosion resistance in many environments. The main copper alloys used in tribology are:

(1) Cu-Zn alloys (at the base of the brass family);
(2) Cu-Sn alloys (conventional bronzes);
(3) Cu-Al alloys (aluminium bronzes);

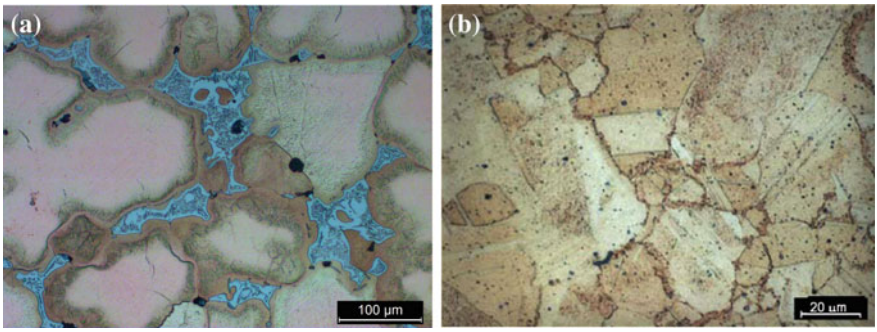

Fig. 6.11 Typical microstructure of an as cast CuSn12 alloy (**a**) [20], and of an extruded Cu-2 % Be-0.5 % (Co + Ni) alloy (**b**) [21]

(4) Cu-Be alloys (beryllium bronzes);
(5) Cu-Ni alloys (nickel bronzes);

Other elements used in copper alloys are lead, manganese and phosphorus, which remains from the refining operation. Copper alloys are used both in the as-cast and wrought condition. They are also easily machined by chip removal. As an example, Fig. 6.11, shows the microstructure of the widely used as cast CuSn12 alloy, and of an extruded Cu-Be alloy. The as-cast alloy is segregated with an interdendritic solidification phase that is made by the α phase, a copper rich solid solution of tin in copper, and the δ phase, an intermetallic compound with composition $Cu_{31}Sn_8$. This latter compound, characterized by a jagged shape in Fig. 6.11a, is hard and brittle. The microstructure of a Cu-2 % Be alloy (containing also 0.5 % Co + Ni), Fig. 6.11b, displays α grains and Co-Be-Ni precipitates (*beryllides*). The matrix hardness is given by a fine dispersion of metastable Cu-Be precipitates.

Copper alloys can be hardened by work hardening and, in some cases, also by heat treatment. The maximum attainable hardness is about 300 kg/mm^2, except for Cu-Be alloys that can reach values around 400 kg/mm^2 after solution treatment and age hardening.

Bronzes are widely used in tribological applications in the case of sliding wear. The coupling between bronzes and steel is characterized by K_a-values as low as 10^{-15} (Table 5.2). This excellent sliding resistance is due to several reasons: the easy formation, during sliding, of a compact oxide layer that is adequately supported by the underlying matrix; the low compatibility between copper and iron that reduces the tendency to adhesive wear (and its contribution when present); the high thermal conductivity that avoids reaching high contact temperatures that could soften the material. For example, by means of dry pin-on-disc tests, it has been obtained that pure copper (H: 102 kg/mm^2) displays a K_a-value of 3.2×10^{-14} m^2/N [22]. When using a age hardenable CuBe alloy (H: 342 kg/mm^2), K_a decreases to 6.16×10^{-15} m^2/N. But when using an age hardenable CuBeNi alloy, characterized by lower hardness (H: 242 kg/mm^2) but higher thermal conductivity, the recorded

K_a was 4×10^{-15} m^2/N. The resistance to adhesive wear is important during the run-in stage and also when wear fragments do not stay in the contact region and thus mild tribo-oxidative wear cannot be fully established.

Bronzes too have good performances under boundary lubrication. In particular, they afford a high resistance to scuffing thanks to their low compatibility versus steel. A typical application is constituted by the coupling between a bronze crown and a hardened helical screw in worm gearing. Here the contact is characterized by prevailing sliding conditions, and a boundary lubrication is attained. Figure 6.12a shows the wear evolution for a cast CuSn12 alloy, during rolling–sliding test carried out at three Hertzian pressures, with a sliding velocity of 3.74 m/s (a synthetic polyglcycolic oil containing anti-scuffing additives was used) [20]. In all cases, a run-in stage was observed. After run-in, wear rate was almost negligible at 260 MPa. At 325 MPa, K_a resulted typical of boundary lubrication. At 350 MPa, after run-in, a steady state stage was firstly observed, but after about 1300 km of sliding, a transition with a noticeable increase in the wear rate was recorded. Such

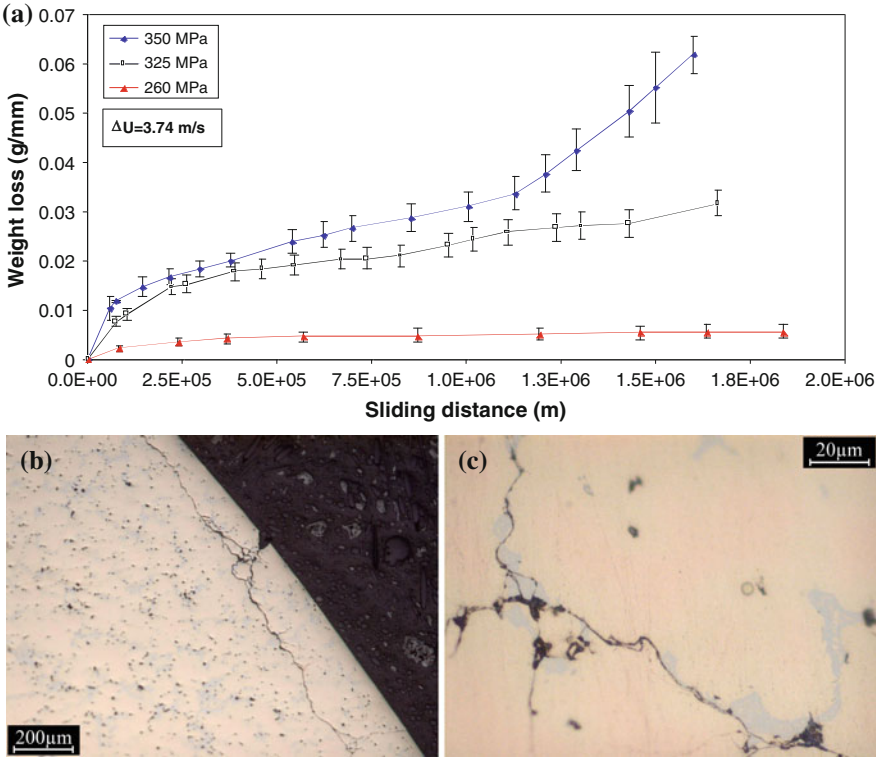

Fig. 6.12 Boundary lubricated rolling-sliding wear test of a CuSn12 cast alloys against a hardened steel (sliding speed: 3.74 m/s; synthetic polyglycolic oil). **a** Wear curves obtained at three load levels; **b** subsurface crack paths; **c** preferential crack path through brittle dendritic phases [20]

an increase was found to be due to the onset of damage by contact fatigue. Surface and sub-surface fatigue cracks were found to nucleate and propagate (Fig. 6.12b, c), aided in this by the brittle inter-dendritic phases rich in tin and lead.

Copper alloys containing lead between 25 and 40 % are widely used in *self-lubricating bearings*. Lead is virtually insoluble in copper (Fig. 1.13), and during sliding it is spread onto the surface by lowering the coefficient of friction, with a mechanism similar to that shown by graphite in grey irons. Better mechanical properties are displayed by lead bronzes (here the amount of lead is usually between 1 and 10 %) or by aluminium bronzes (5–11 % Al). These alloys are suitable for the realization of bearings loaded by high nominal pressures (above 1 MPa) or for the manufacturing of gears. Similar to the Cu-Sn-Al alloys are the Cu-Sn-Mn alloys, containing up to 1 % Mn.

A special mention deserve the so-called *beryllium bronzes* (Cu-Be alloys), which can be precipitation hardened if the concentration of beryllium is greater than 1.3 %, thus achieving a tensile resistance comparable to that of steels. The high mechanical strength and corrosion resistance, both in marine and several industrial environments, make them particularly suited for power gears. Figure 6.11b shows the microstructure of a typical Cu-Be alloy. Different Cu-Be alloys are available from the market. In general, as alloying is increased, mechanical strength is also enhanced whereas thermal conductivity is decreased. Therefore, the optimal alloy composition can be selected on the basis of the required performances.

A particular class of bronzes are those obtained by *powder metallurgy*. They have a typical content of tin around 10 % and, most importantly, they usually contain up to 10 % of residual porosity that provides self-lubricating properties. The porosity, in fact, is infiltrated with lubricant, which expands during operation as temperature increases and spreads between the mating surfaces. In this way, the lubricant ensures a typically mixed lubrication [23]. In order to prevent the occurrence of adhesive wear during the run-in stage, i.e., when the oil is still leaking from the pores, 1–3.5 % graphite is added to the material.

Finally, *phosphor bronzes* are mentioned. They are particularly important for applications (such as gears) where contact fatigue under mixed or boundary lubricated conditions is encountered. Phosphorus forms hard precipitates with copper carrying the contact load, whereas the surrounding softer matrix is worn thus forming reservoirs for the lubricating oil [24]. These materials have a hardness of around 100 kg/mm^2 and may have a fatigue strength (for a life of 10^7 cycles) above 400 MPa.

6.4 Aluminium and Titanium Alloys

Aluminium and titanium alloys are characterized by attractive engineering properties. Both have a relatively low density (around 2.7 g/cm^3 for aluminium alloys and 4.5 g/cm^3 for titanium alloys) and high corrosion resistance in many aggressive environments. Titanium alloys are also biocompatible, and can be used as

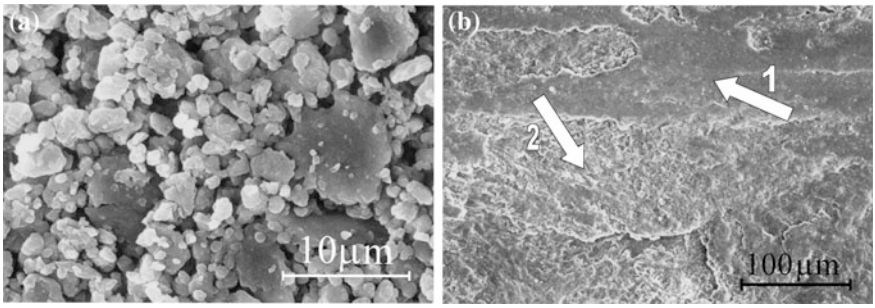

Fig. 6.13 Morphology of the wear debris (**a**) and of the worn track (**b**) in the case of an Al-7072 alloy after dry sliding at 1 MPa and 0.2 m/s against a 52100 steels [27]. The tribolayer is very compact and dense in some regions (see *arrow 1*), whereas it is rather fragmented in others (see *arrow 2*)

orthopaedic and osteosynthesis materials. However, albeit for different reasons, both have a limited resistance to nearly all wear mechanisms.

Aluminium alloys are characterized by a relatively low hardness (they reach hardness values of about 250 kg/mm^2) that considerably decreases as temperature increases. Aluminium alloys, in fact, begin intense thermal softening at a temperature around 100 °C. Consequently, at this temperatures both their friction coefficient and specific wear coefficient start to noticeably increase. The transition from mild tribo-oxidative wear to severe adhesive wear occurs at relatively low values of applied pressure and sliding speed. It has to be further noted that the protective action of alumina, which is at the basis of tribo-oxidative wear, is not as efficient as, for example, the Fe-oxides in steels, since it does not display any ductility, i.e., any ability to spread onto the wear surface. Moreover, its adhesion to the substrate is low [25]. In Al-alloys the protective layer that is formed under tribo-oxidative wear is typically a mixture of oxides originating also from the counterface. As an example, Fig. 6.13 shows the morphology of the wear debris (a) and of the worn track (b) in the case of an Al-7072 alloy after dry sliding at 1 MPa and 0.2 m/s against an AISI 52100 steel [26]. The fragments appear to be small and equiaxed; they originate from the brittle fragmentation of the tribolayer, i.e., from regions 2 in Fig. 6.13b, that is formed by aluminium and iron oxides.

In aluminium alloys adhesive wear is particularly severe, since it is characterized by intense transfer phenomena. These alloys are then unsuitable for sliding applications that may give rise to relatively high contact temperatures. For example, they are poorly suitable for non-conformal contacts, which are typically characterized by high contact pressures [27]. Aluminium alloys are therefore mainly used in conditions of conformal contact, such as in *sliding bearings*, that work under relatively mild loading conditions. A common alloy used in plain bearings is the Al-20 % Sn alloy, consisting of a ductile phase (tin, practically insoluble in aluminium) in a relatively hard matrix. Lead can be also added in place of tin.

The sliding resistance of aluminium alloys can be enhanced by reinforcing them with ceramic particles. *Aluminium matrix composites* typically contain 20 % of alumina or SiC particles. The presence of these particles shifts the boundary between mild tribo-oxidative wear and severe adhesive wear to higher nominal pressures and sliding speeds [28]. These composites, however, are still quite expensive, especially for the complex production process they require. Another method that can be employed to improve the sliding wear resistance of aluminium alloys, consists in growing a surface layer of aluminium oxides by hard anodizing or in the deposition of thin films (Chap. 7).

Titanium alloys also show a poor wear resistance, although they may posses high mechanical strength and they do not undergo thermal softening as aluminium alloys (note that titanium has a melting temperature of 1670 °C compared to 660 °C of aluminium). In case of dry sliding wear, titanium alloys show typical K_a-values that are around 10^{-13} m^2/N, even if the wear mechanism is tribo-oxidation [29]. This is due to several reasons: titanium oxides possess low protection properties since the ratio between their specific volume and that of the metal is less than 1. In addition, the oxides are not adequately supported by the underlying material that, during sliding, it is not able to strain-harden enough. Indeed, it undergoes considerable plastic deformation that localizes easily in shear bands that weaken the microstructure [30]. This last tendency my also promote intense material transfer during adhesive wear, making seizure quite easy to occur.

Also for titanium alloys various surface treatments have been proposed to improve wear resistance, including thermal oxidation (like aluminium, titanium displays a high affinity for oxygen), anodizing, nitriding, ion implantation, or the deposition of ceramic coatings, which will be presented in the next chapter. It is worth noting that thermal oxidation is a simple and cost effective treatment, able to reduce the friction coefficient and the wear rate in different tribological systems. However, the thickness and compactness of the oxide layer has to be optimized since it is quite brittle and shows a tendency to damaging and removal even at quite low applied loads [31].

Another method for reducing friction and wear in sliding or sliding-rolling is the use lubrication. However, in titanium alloys the use of conventional lubricating oils is not quite effective, and specific research is still ongoing for the development of lubricants that could be suitable for these alloys. Table 6.4 shows the experimental results of tribological tests carried out in a disc-on-disc configuration using discs made of the Ti-6 % Al-4 % V alloy (with a hardness of 350 kg/mm^2 and a yield strength of 900 MPa) and a common SAE 15 W/40 lubricating oil [32]. At a

Table 6.4 Results of rolling-sliding tests (10 % sliding) performed using Ti-6 % Al-4 % V discs, lubricated with common SAE 15 W/40 oil (data from [32])

Hertzian pressure, MPa	Λ factor	Coefficient of friction	Wear
640	0.4	0.065 (0.3)	Scuffing
320	0.5	0.034	$K_a = 2.64 \times 10^{-15}$ m^2/N
226	0.6	0.034	$K_a = 2.12 \times 10^{-15}$ m^2/N

Hertzian pressure of 640 MPa, the coefficient of friction was initially around 0.065, but, soon after, a transition to a much greater value, around 0.3, was observed. This is a typical value for dry sliding. As a matter of fact, after the transition wear became particularly intense with values of K_a around 10^{-14} m^2/N. This result is quite unexpected since at this load level the ratio p_{max}/τ_Y is very low (less than 2). In this condition, steels would show a contact fatigue life in excess of 10^8 cycles. The observed transition was caused by scuffing. In fact, during the initial stages of the test, the thin natural surface oxide layer (1.5–10 nm thick) is removed since lubrication is mixed ($\Lambda = 0.4$). As a consequence, the lubricant is no longer able to properly wet the surface of the metal, since the ionic bonds of the oxide layer favour the anchoring of the polar molecules of the lubricant, and scuffing may start. The low thermal conductivity of titanium and its alloys (around 6.7 W/mK) plays clearly an important role in favouring the onset and propagation of scuffing.

In the tests at lower Hertzian pressures, scuffing was not observed. However, wear was still present and the specific wear coefficient went up to around 2×10^{-15} m^2/N, which is about two orders of magnitude lower than the typical value for dry conditions. This means that a boundary lubrication regime was attained during the tests, even if the lambda factor was around 0.5–0.6, a typical value for mixed lubrication. Again, this behaviour is due to the poor wettability of titanium alloys by lubricating oils.

6.5 Advanced Ceramics

Several *natural ceramics*, such as rocks (silica or aluminosilicates), marble (mainly made of calcium carbonate), or *traditional ceramics*, such as glass, clay products and concrete, have been used for centuries, and are used also today, for tribological applications, such as in floors or as grinding tools. In the past decades, the so-called *advanced ceramics*, such as *alumina*, *zirconia*, *silicon nitride*, *silicon carbide* and *sialon* (containing alumina and silicon nitride in different compositions), have been developed. They are ideal for wear resistant applications, thanks to their high hardness, high chemical inertness in many environments, and low density. In particular, their ability to retain high hardness at high temperatures, as shown in Fig. 6.14, is particularly important in tribology.

However, all ceramics possess quite low fracture toughness, typically around 5 MPa $m^{1/2}$, and can display brittle contact and wear by brittle fragmentation. To minimize this problem, advanced ceramics are produced in a very controlled manner, in order to reduce the content of defects, especially on the surface. In addition, special ceramic composites have been also developed, containing toughening phases in their microstructure or having laminated structures designed to induce compressive stresses at the surface. It is clear that the use of highly controlled production routes and/or special materials has a significant impact on the manufacturing costs. Therefore, it is often preferred to deposit a ceramic layer on a different substrate, such as a metal, which is less expensive and is also tougher.

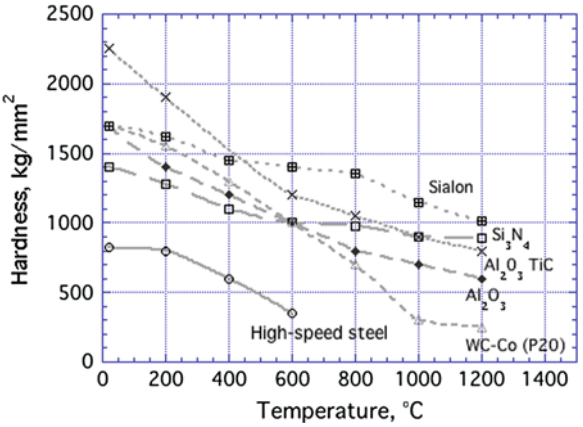

Fig. 6.14 Hardness as a function of temperature for different advanced ceramics and, for comparison, for WC-Co hardmetal, and a high-speed steel (from different literature sources)

Monolithic advanced ceramics are typically produced by powder routes; the most used techniques are liquid phase sintering, hot isostatic and dry pressing, injection moulding and slip casting. With these techniques, finished components with complex shapes can be manufactured. Standard parts with simple geometries, e.g. plates or bars, are also produced. They can be then machined and assembled together and/or with metallic parts to obtain the final part [27].

Table 6.5 lists some advanced ceramics that are used in tribological applications, along with relevant physical-mechanical properties. In the table, the constant β is also included. It expresses the dependence of the material hardness on temperature according to the following relationship:

Table 6.5 Physical and mechanical properties of some advanced ceramics (data obtained from different literature sources)

Material	Density (g/cm^3)	Elastic modulus (GPa)	Hardness (kg/mm^2)	β (10^{-4}, °C)	K_{IC} (MPa $m^{1/2}$)	Thermal shock resistance (ΔT_c, °C)
Alumina (Al_2O_3)	3.9	380	1700	8.5	2–4	200
Partially stabilized zirconia (PS ZrO_2)	5.8	200	1300		10	500
Sialon ($Si_3Al_3O_3N_5$)	3.2	300	1430–1850	4.4	6–7.5	510
Silicon nitride (Si_3N_4)	3.2	310	1400	3.8	4	700
Silicon carbide (SiC)	3.2	410	3100	10	4	300–400

$$H = H_0 \cdot e^{-\beta T} \tag{6.2}$$

where T is the temperature in °C, and H_0 is the hardness at room temperature. It should be noted that all the listed values are only indicative, because the materials properties depend very much on the manufacturing process and on the compositional characteristics (such as the residual porosity, grain size, purity, and so on).

Advanced ceramics are particularly suitable in applications characterized by sliding wear and low-stress abrasive wear. Examples include cutting tools, sealing rings, manufacturing dies, which are mainly made by alumina, or zirconia when some fracture toughness is required, as in presence of impacts. Other examples are ball bearings (especially operating at high temperature) and engine valves, which are mainly made by silicon nitride or silicon carbide [33]. Ceramic particles are also used as abrasives for grinding wheels.

6.5.1 Sliding Wear

In case of dry sliding against a steel counterface, the specific wear coefficient, K_a, of ceramics is quite low, typically between 10^{-16} and 10^{-15} m^2/N (see Table 5.2). In the case of couplings between ceramic materials, K_a can vary between 10^{-12} and even 10^{-18} m^2/N. Therefore, by a proper selection of a tribological pair it is possible to achieve very low wear rates. The dry sliding behaviour of ceramics is characterized by three main damage mechanisms [34, 35]:

(1) For small loads and low sliding speeds, wear is mild and K_a typically assumes values that are less than 10^{-15} m^2/N. During running in, the brittle fragmentation of the highest asperities produces wear debris that are compacted and possibly oxidized during sliding, forming protective scales such as those shown in Fig. 2.14. As a consequence, wear is mild and possibly by tribo-oxidation.
(2) As load is increased, a transition to severe wear may occur. Wear is dominated by macroscopic brittle contacts, with the formation of wear fragments due to the propagation of cracks under the action of the surface tensile stress originated by friction (see Sect. 4.1.2). The fracture is often intergranular, as shown, again, in Fig. 2.14.
(3) At high sliding speeds, a transition to severe wear may occur even if the contact stresses are relatively small. In fact, the low thermal conductivity of ceramics favours the attainment of high flash temperatures. They can induce the formation of surface tensile thermal stresses that may in turn form surface cracks, which then produce wear fragments.

The possibility of having severe wear of type (2) is lower in materials with high fracture toughness (see Eq. 4.3), while the possibility of having severe wear of type 3 is lower in materials with high *thermal shock resistance*. The thermal shock resistance is expressed by the critical temperature interval, ΔT_c, the material can

withstand without breaking. In a simplified view, an abrupt temperature change, ΔT, can induce a tensile stress given by

$$\sigma_t = E \cdot \alpha \cdot \Delta T \tag{6.3}$$

where α is the coefficient of thermal expansion. To estimate ΔT_c, the relation 1.10 can be used:

$$\Delta T_c \approx \frac{K_{Ic}}{1.12 \cdot E \cdot \alpha \cdot \sqrt{\pi c}} \tag{6.4}$$

where c is the size of a pre-existing surface microcrack that may trigger the brittle fracture. As mentioned in Sect. 4.1.2, c is most often equal to the grain size. Typical values for ΔT_c are included in Table 6.5.

It is therefore clear that the materials with the largest values of both K_{Ic} and ΔT_c are those with the best sliding wear resistance, since the transition to severe wear is displaced to high Hertzian pressures and high sliding speeds. From Eq. 4.3, it is obtained that the transition to type (2) severe wear is avoided if:

$$\frac{(1 + 10\mu) \cdot p_{\max} \sqrt{d}}{K_{Ic}} \leq 3 \tag{6.5}$$

where d is the average grain size. It has been obtained that the transition to type (2) severe wear is avoided if [36]:

$$\frac{\gamma \mu}{\Delta T_c} \sqrt{\frac{v F_N H}{k \rho c}} \leq 0.04 \tag{6.6}$$

where γ is here the fraction of heat that enters the sliding body (it is defined by Eq. 2.23). Table 6.6 shows the experimental transition values for the Hertzian pressure and sliding velocity in the case of Al_2O_3/Al_2O_3 and SiC/SiC pairs, obtained using a pin-on-disc test in a sliding point contact [36].

To complete the picture, it has to be considered that sliding wear of ceramics is also affected by ambient *humidity*. If it is increased, it may induce a decrease in K_{Ic} thus favouring wear. Most importantly, humidity may interact with the ceramic surface and produce oxide/hydroxide molecules by tribochemical reactions. Such

Table 6.6 Transition values for the Hertzian pressure and sliding speed from mild to severe wear for two ceramic pairs

Coupling	Hardness (kg/mm^2)	Hertzian pressure (MPa)	v (m/s)
Al_2O_3/Al_2O_3	1660	≈1820	≈0.3
SiC/SiC	3140	≈1600	≈1.5

Data obtained with a pin-on-disc test, operating in dry sliding and in a point contact (data from [36])

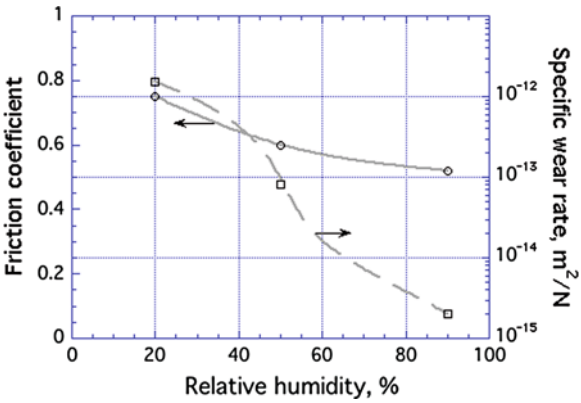

Fig. 6.15 Experimental dependence of friction and wear on the ambient humidity, in case of the SiC/SiC coupling (modified from [38])

molecules may act as soft lubricants, reducing both friction and wear (see also Sect. 2.6) [37]. These effects have been throughout recorded in alumina, silicon nitride and silicon carbide. Figure 6.15 shows, as an example, the experimental dependence of friction and wear on the ambient humidity, in case of the SiC/SiC coupling [38]. The same beneficial effects are obtained in the case of sliding in water [39]. It is also reported that the formation of a tribochemical layer on ceramics may greatly help with water lubrication, improving in this respect wear resistance of mechanical parts that operate in the presence of water, such as seals or bearings in water pumps.

A reduction of the transition pressure from mild to severe wear is typically observed as temperature is increased up to 300–500 °C, as shown in Fig. 6.16 for an alumina/alumina coupling. This is mainly due to the increase in the friction coefficient (see Eq. 6.5), due to the desorption of the tribochemical layer. However, at particularly high temperatures, i.e., above about 800 °C, wear becomes mild again. As shown in Fig. 2.21, at these temperatures the incipient melting of the sintering additives and impurity inclusions, mainly those at the grain boundaries, takes place.

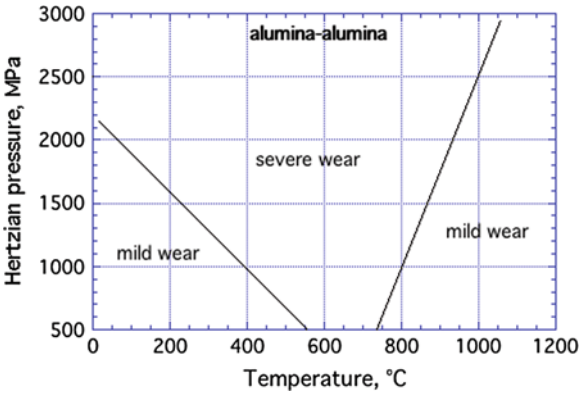

Fig. 6.16 Influence of ambient temperature and Hertzian pressure on the dry sliding behaviour of the alumina/alumina pair (obtained from different literature data)

It causes the formation of a glassy layer that reduces friction and, in turn, makes more difficult the transition to severe wear. To further reduce wear at high temperatures, solid lubricants such as MoS_2 can be employed.

6.5.2 Wear by Contact Fatigue

Silicon nitride, typically produced by hot isostatic pressing, is currently used in the production of balls and rolls for rolling bearings, especially of the hybrid type, i.e., bearings having a steel raceway. These bearings are particularly suitable in extreme applications, such as at high temperature and/or high speed (the low density of the material reduce the centrifugal forces). It has been verified that rolling bearings made of silicon nitride can be effectively lubricated using mineral oils, obtaining a lubrication degree that is similar to that found in steel components. The contact fatigue life of these materials is comparable or superior to that of the best bearing steels [40]. In order to reduce the possibility of surface nucleation of fatigue cracks, all ceramic parts must be carefully produced with a very low roughness and low defectiveness, such as the residual pores or grinding cracks, which should be smaller than 2 μm (see Sect. 8.10).

6.5.3 Abrasive Wear by Hard, Granular Material

Ceramics are particularly suited for applications with low-stress abrasion such as in conveyors of mineral particles where alumina is widely used. Ceramics are also used in the case of erosive wear, when both the impact velocity and the impact angles are relatively low (Table 5.8). For example, alumina and silicon carbide (with higher hardness than alumina) are used for gas turbine parts, sinter plants, sealing bearings, powdered coal lines, just to mention some applications where high erosion resistance, even at high temperature, is required [41]. In general, the erosion rate typically increases with temperature. As an example, Fig. 6.17 shows the erosion rate as a function of temperature for a silicon carbide and a silicon carbide-titanium diboride composite [42]. The tests were conducted using silicon carbide particles as erodent, with a particle velocity of approximately 70 m/s and an impact angle of 90°. The wear increase with temperature is consistent with the Lawn and Swain mechanism (Fig. 1.7). In fact, as temperature rises, the materials hardness is lowered, the plastic zone at the contact is larger and the residual stresses that drive lateral crack propagation are also larger. However, it should be noted that the erosion rate of ceramics also depends on the product: $H^n K_{Ic}^m$, where $n = -0.15$ and $m = -1.3$ [43]. As temperature is increased, the erosion rate may remain unaffected or even decrease if the fracture toughness increase with temperature has an overwhelming effect.

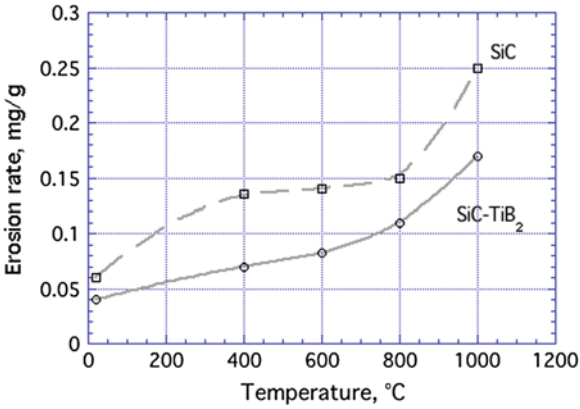

Fig. 6.17 Erosion rate as a function of temperature for a silicon carbide and a silicon carbide-titanium diboride composite (modified from [42])

6.6 Cemented Carbides

Cemented carbides, also called *hardmetals* or *cermets*, have been developed with the objective of obtaining ceramic materials with improved fracture toughness. These materials are produced by sintering powder mixes of metal carbides, such as WC, TiC and TaC, and about 3–30 % of metal powder, such as cobalt or nickel. During sintering, the metallic powder melts forming a liquid film that wets the carbide particles thus activating the sintering process. The result is a material characterized by high hardness and stiffness, coupled with a fracture toughness of about 15 MPa $m^{1/2}$, i.e., definitely larger than that of advanced ceramics. This is because the metallic film (also called: *binder*) renders more difficult both crack nucleation and propagation.

Most cemented carbides contain tungsten carbides in a cobalt matrix. Materials containing different fractions of other carbides, such as TiC and TaC (the so-called *ternary carbides*) are also produced. Table 6.7 summarizes some types of cemented carbides, indicated with the ISO designation, with their compositions and main mechanical properties. It can be noted that these materials display high hardness, high values of the elastic modulus (it is about three times that of steel), and a high density.

Table 6.7 Composition and mechanical properties of some common cemented carbides

Designation ISO	WC (%)	TiC + TaC (%)	Co (%)	Density (g/cm^3)	Hardness (kg/mm^2)	Elastic modulus (GPa)
P20	79	13	8	12.1	1580	530
P40	85	5	10	13.4	1420	540
K20	94		6	14.8	1650	610
K40	89		11	14.1	1320	560
M20	82	10	8	13.3	1540	560
M40	86	6	10	14	1380	530

In general, as the metallic fraction is increased, fracture toughness also increases whereas hardness decreases. Therefore, the selection of a suitable cemented carbide depends on the design requirements. Another important microstructural parameter is the average carbide grain size. It is typically between 1 and 6 μm, but also submicron (0.5–0.8 μm), ultrafine (0.2–0.5 μm) and nano (<0.2 μm) powders can be used. Generally speaking, as grain size is decreased, hardness is increased without penalizing fracture toughness.

Cemented carbides possess excellent resistance to sliding wear and to abrasion wear, even at high temperatures. They are commonly used in the construction of machining tools, sliding bearings, seals, components or parts subject to abrasive wear, chains, rolls for rolling, punches for moulding plates, matrices for extrusion. Two limitations characterize these materials: the low formability and the high cost. It is then necessary to fully exploit the potentiality of powder metallurgy for producing near net shape components. The allowed machining processes are electro-discharged machining (EDM) and grinding. Because of this, cemented carbides are often deposited as surface layers by the HVOF technique (Fig. 7.18).

6.6.1 Sliding Wear

Cemented carbides display a very high sliding wear resistance. Table 5.2 shows that they are characterized by K_a values around 5×10^{-16} m^2/N when dry sliding against steel. In general, wear rate decreases as hardness is increased, i.e., as the amount of metallic binder and the average carbide grain size are decreased. Figure 6.18 shows the experimental dependence of hardness and K_a with the binder content, for a WC-Co hardmetal with a carbide grain size of around 1 μm, dry sliding against steel (H: 200 kg/mm^2) [44]. It has been observed that wear was characterized by the progressive removal of the cobalt binder, accompanied by the brittle fracture and fragmentation of the carbide grains.

As shown in Fig. 6.14, cemented carbides are able to retain a relatively high hardness also at high temperature. Therefore, they are also used in dry sliding,

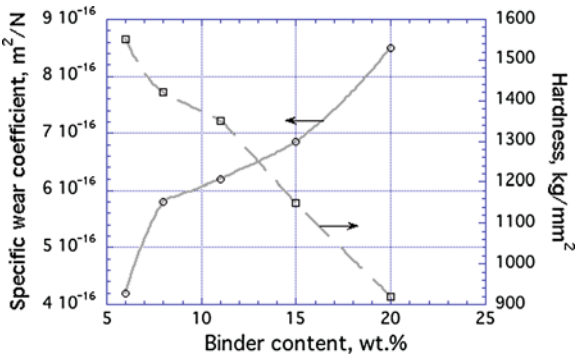

Fig. 6.18 Specific wear coefficient and hardness versus binder content in case of WC-Co dry sliding against a steel counterface (modified from [44])

where high temperatures are reached in the contact regions, such as in cutting tools. Under these conditions these materials exhibit excellent wear resistance when mating cast iron or non-ferrous alloys, but they do not afford a good performance in sliding against steel. In fact, at high contact temperatures (above 800 °C) tungsten carbide grains decompose and then carbon diffuses easily into the austenitic steel phase of the counterface (the chip in case of cutting tools). This leads to a considerable reduction in mechanical strength with a corresponding increase in adhesive wear. However, it has been verified that the addition of titanium and tantalum carbides significantly increases the wear resistance, because these carbides are more stable at high temperature.

6.6.2 Abrasive Wear by Hard, Granular Material

Cemented carbides display a high abrasion resistance under low-stress as well as high-stress abrasion (Sect. 5.4). Figure 6.19 shows the results of abrasion tests carried out using silica particles in the size range 125–180 μm and a testing apparatus similar to the DSRW (but using a metal wheel without a rubber rim) [45]. The results are in the typical range of low-stress abrasion, and highlight the role of the fraction of binder and, most importantly, the role of the grain size. In particular, it is noted that the specific wear rate is very low when the grain size is below 1 μm. Authors observed that the ultrafine grades behave as a one-phase material, without the fragmentation and displacement of the individual WC grains during the abrasive interaction. Ultrafine materials were obtained by sintering nanocrystalline powder produced by the spray conversion process and contained 0.8 % vanadium carbide as grain growth inhibitor.

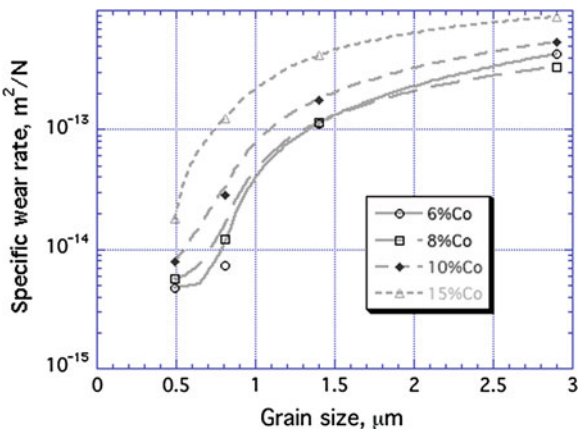

Fig. 6.19 Effect of grain size and binder content on the abrasive wear resistance of WC-Co cemented carbides (modified from [45])

6.7 Graphite and Diamond

Graphite and diamond are two allotropic forms of carbon. They are characterized by very different properties but both are quite important in tribology.

Graphite has the crystal structure shown in Fig. 3.2a. The adsorption on the carbon planes of molecules from the external environment, such as water vapour, provides this material the capability of a solid lubricant. As a solid lubricant, graphite is typically employed as a powder (Sect. 3.1.1). In many applications it is also used as monolithic component. In this latter case, the process route consists in mixing fine natural coal or coke with natural graphite (in the typical ratio 80/20) together with pitch. The mix is then extruded or compression moulded to obtain finished parts with simple geometry, or blanks such as rods, plates and tubes to be further machined and assembled. The products are sintered at about 1000 °C, and the remaining porosity is removed by hot isostatic pressing or it is impregnated with a phenolic resin or a metal.

The main properties of graphite are:

- Low density (about 1.8 g/cm^3);
- Low hardness (less than 100 kg/mm^2);
- Low elastic modulus (between 15 and 20 GPa, depending on the porosity content;
- High thermal conductivity (which varies from 20 to 180 W/mK, and can even reach values of 400 W/mK in products with a high graphite content).

The properties of industrial graphite depend much on the characteristics of the starting materials and the production route. For example, by sintering at high temperature (above 2500 °C) and for long times, the degree of graphitization is increased, and materials with increased thermal conductivity are obtained [1].

Industrial graphite is employed in several tribological applications characterized by sliding wear, quite often in dry conditions. The extruded grades are mainly used in dry bearings and electrical bushes (Table 5.3), while the compression moulded grades are mainly employed in more demanding applications, in terms of applied load and sliding velocity, like mechanical seals, piston rings and vanes in vacuum pumps and compressors. The surface hardness of graphite can be increased by a silicon enrichment to form silicon carbide. The siliconized grades are used, for example, in the production of braking parts in racing applications. For high temperature applications, the so-called *carbon-carbon composites* are also produced. They are made from graphite reinforced with carbon fibres, and are widely used in the production of aircraft braking parts, and also for special aerospace applications and in the glass industry.

Since the materials usually contain up to 15 % of abrasive ash, graphite has to be coupled with sufficiently hard surfaces, such as hardened steel (with hardness typically greater than 500 kg/mm^2), chromium plated materials, materials coated with advanced ceramics such as silicon carbide. At relatively small loads and low sliding velocities, sliding wear (by adhesion) is mild and the friction coefficient is

low. Typical values of friction coefficient are in the range 0.06 and 0.2, and the specific wear rate is around 10^{-15} m^2/N. If the contact temperature reaches a critical value of about 350 °C, the surface desorption of the water molecules takes place and the so-called *dusting wear regime* is entered. The friction coefficient increases to 0.4–0.5, and also wear rate increases [40]. For the estimation of contact temperature, it has to be considered that the specific heat of graphite ranges between 0.71 and 0.83 kJ/kg °C, and is around 1.4 kJ/kg °C for carbon-carbon composites [46].

Diamond is characterized by the highest hardness (up to 10,000 kg/mm^2) of all known materials, the highest modulus of elasticity (around 1000 GPa), the highest thermal conductivity (around 2000 W/m °C) and the lowest coefficient of thermal expansion (0.8×10^{-16} $°C^{-1}$) [47]. In industrial applications, the synthetic *polycrystalline diamond* (also referred to as PCD) is typically used. PCD powders are obtained from graphite, by heating it at high temperature and high pressure in the presence of a catalyst. Diamond powder is used as a super-abrasive in grinding and polishing. It may be also sintered with metallic binders (such as cobalt and nickel) to obtain particular parts, such as machining tools where PCD is typically sintered on a hard metal. The applications of PCD machining tools are substantially similar to those of cemented carbides, with the difference that the high hardness allows working extremely abrasive materials, such as metal matrix composites and ceramics. PCD tools are also not suitable for cutting ferrous alloys, since the high contact temperatures allow carbon to diffuse into the ferrous alloy that is typically austenitic, and the tool may be severely damaged.

The polycrystalline diamond is also produced as a coating by CVD (Chemical Vapour Deposition). During deposition, the temperature of the substrate is variable between 700 and 1000 °C. The coatings cannot be realized on steels since the deposition temperature is too high. They are typically realized on cemented carbides. A limitation for the use of these coatings is given by the poor adhesion with substrate that can be improved by suitable surface treatments before diamond deposition, such as mechanical scratching or chemical etching to remove the cobalt from the surface in the case of deposition on Co-based cemented carbides [48]. Another possible limitation is given by the high surface roughness, due to the faceted morphology of the coatings (Fig. 6.20 shows an example).

The polycrystalline diamond is characterized by a very low coefficient of friction (between 0.02 and 0.05) in the case of dry sliding against itself or a ceramic material. Figure 6.21 shows the evolution of friction coefficient in the case of dry sliding of a PCD against granite. The tests were conducted in a block on ring configuration, at three loads: 200, 400 and 600 N. It is noted that during a short running in stage the friction coefficient is higher than 0.1 but then it decreases reaching very low values. Such low values are determined by a combination of high hardness and low surface energy. It is believed that the low surface energy of PCD, which gives rise to a low work of adhesion, is due to adsorption of water molecules from the external environment [40]. The specific wear rates are also very low, between 10^{-17} and 10^{-16} m^2/N.

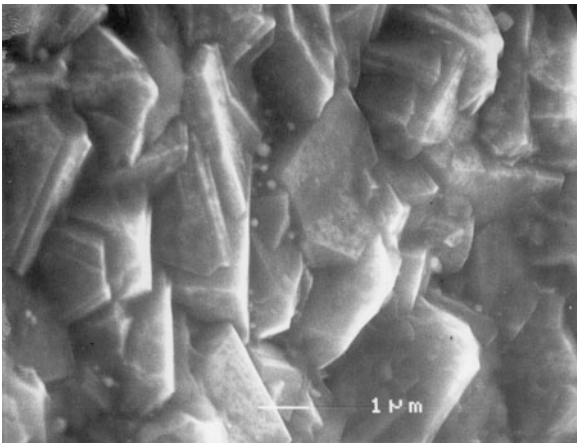

Fig. 6.20 SEM micrograph showing the faceted morphology of a CVD PCD deposited on WC-Co [48]

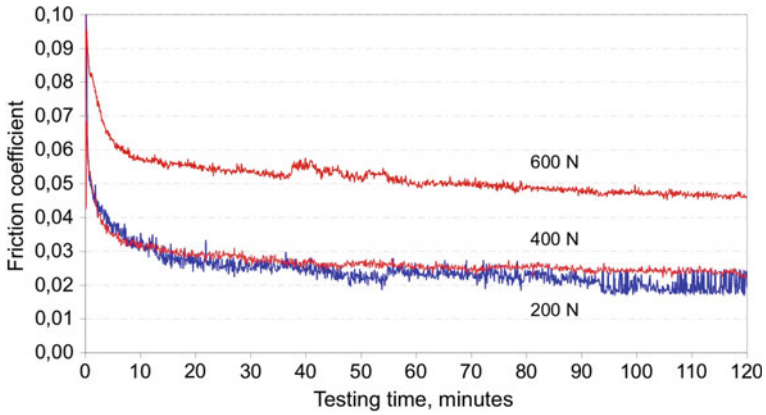

Fig. 6.21 Evolution of the friction coefficient in the case of dry sliding of a PCD against granite

6.8 Polymers

Polymeric materials are widely used in tribology, especially in applications where dry sliding wear occurs (in particular against a metal counterface). They are often produced with the addition of short fibres or particles, to increase their strength, or to provide them with self-lubricating properties. Among the advantages of using polymers are: low compatibility versus metals (due to the low surface energy), high chemical inertness in several aggressive environments, self-lubricating properties, low density (around 1 g/cm^3), ability to absorb vibrations and shocks. In addition,

polymers can be quite easily shaped, mainly by extrusion and injection moulding. Semi-finished rods, tubes, plates and sheets are also produced, and they are easily machined and joined together. Examples of applications include plain bearings (typically operating in the absence of lubrication), various types of gears (with the additional characteristic of being little noisy due to their damping capability), piston rings (running dry), seals, biomedical applications (several polymers show excellent biocompatibility). In comparison to metals, polymers have the disadvantage of a lower strength (partially limited by the use of reinforcements) and a lower temperature resistance.

Polymers are divided into two groups: *thermoplastics* and *thermosets*. Thermosetting polymers are stronger and stiffer than thermoplastics but they do not show a melting phenomenon and are more difficult to process and shape. Thermosets include phenolic materials, epoxy resins and polyimides. Thermoplastic polymers are most widely used in tribological applications. In the solid state they can be *amorphous* or *partially crystalline*. Figure 6.22 provides a schematic representation of the main mechanical properties of thermoplastics with respect to temperature (T_g: glass transition temperature; T_f: melting temperature), in the case of amorphous polymers and 100 % crystalline polymers (partially crystalline polymers display intermediate behaviour). Depending on the position of T_g (and T_f) with respect to room temperature, four classes of materials can be recognized:

- A: Amorphous materials with high T_g-values (including polycarbonate, PC, with T_g = 150 °C, and polymetyl methacrilate, PMMA, with T_g = 105 °C). At room temperature they are mainly hard and brittle since room temperature is far below their T_g. These polymers display brittle behaviour since their chains are interlocked, making plastic flow difficult. In the presence of surface cracks, these materials exhibit brittle contact.

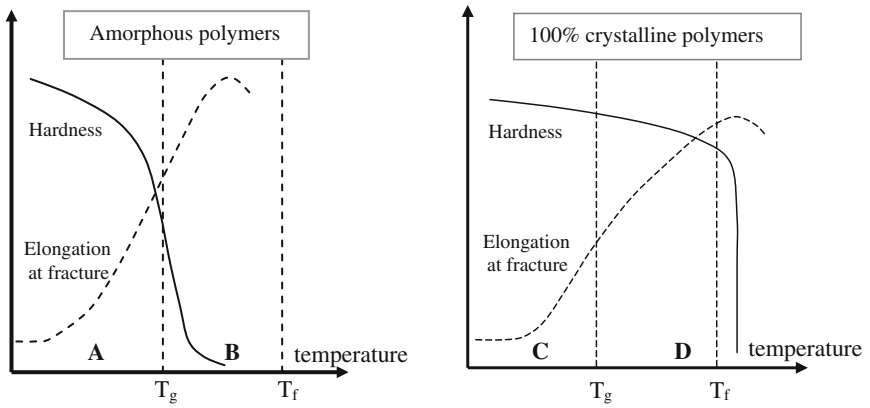

Fig. 6.22 Effect of temperature on hardness and ductility of polymers. Regions *A*, *B*, *C* and *D* identify four classes of polymers that at room temperature show a distinctive mechanical behaviour (see text for more details)

- B: Amorphous materials with low T_g-values (including rubber with $T_g = -73$ °C). At room temperature they are largely above their T_g and they are therefore very soft and display high fracture strain.
- C: Partially crystalline materials with high T_g-values (including polyamides, PA, like Nylon 66 with $T_g = 55$ °C, polyether ether ketone, PEEK, with $T_g = 148$ °C). At room temperature they are quite hard and strong, and they fracture at a limited elongation (of the order of 5 %). These materials my give brittle contact at low temperature.
- D: Partially crystalline materials with low T_g-values (including high-density poliethylene, HDPE, with $T_g = -100$ °C, polyoximethylene, POM, with $T_g = -80$ °C and typically a low content of amorphous phase, polytetrafluoroethilene, PTFE, with $T_g = -90$ °C). At room temperature they are quite hard and ductile. They typically give a viscoplastic contact.

The most common polymers employed in tribology are: polyamide (PA, like Nylon 66); polyacetals or polyoximethylene (POM); polytetrafluoroethilene (PTFE); high-density poliethylene (HDPE) and ultrahigh molecular weight polyetylene (UHMWPE); polyimide (PI). In most engineering applications they are employed with the addition of different types of particles or short fibers, i.e., in the form of *composites*. Table 6.8 lists some characteristics of polymers used in tribology. The data are only indicative because they may vary greatly depending on the type of polymer and production process.

6.8.1 Sliding Wear

Polymeric materials display a high sliding wear resistance against metals, and in particular against steel, as long as the contact temperature remains sufficiently low to allow the establishment of mild wear regime (Sect. 5.1.2). The coupling between polymers and metals is characterized by a low tribological compatibility. Moreover, metals possess a relatively high thermal conductivity that helps in reducing the contact temperature. However, the initial roughness of the metal counterface has to be properly optimized in order to minimize wear, as already seen for the friction coefficient (Sect. 2.9). An example of the experimental dependence of K_a on surface roughness of the steel counterface is shown in Fig. 6.23a for Nylon 66 [17]. In general, optimal R_a-values are between 0.2 and 0.4 μm.

Figure 6.23b shows the specific wear rate of a Nylon 66 as a function of sliding speed [49]. A transition from mild to severe wear is observed at a sliding velocity of around 10 m/s, in correspondence of which the contact temperature reaches the critical value of 250 °C that causes an excessive softening of the material. As shown in Sect. 2.11, different parameters determine the contact temperature between two sliding bodies: sliding speed, applied pressure, friction coefficient, counterface material, ambient temperature and system geometry. Figure 6.24 shows the dry sliding wear map of a polyimide containing 15 % of graphite, obtained using a

Table 6.8 Main characteristics of some polymers widely used in tribological applications

Material	Density (g/cm^3)	Elastic modulus (GPa)	Maximum operating temperature (°C)	K_a (m^2/N)	Observations
HDPE	0.96	0.4–1.2	120	10^{-14} to 10^{-15}	Used for piping, toys, houshold ware
					UHMWPE is used in orthopedic implants
Polyamide (nylon 66)	1.14	3.3	180	10^{-14} to 10^{-15}	Widely used in gears, bearings, bushes
Polyamide + graphite	1.2	4	180	$\approx 10^{-15}$	Graphite reduces friction and wear
Polyacetal (POM)	1.4	2.9–3.3	140	$\approx 10^{-15}$	Excellent dimensional stability; high mechanical properties; recommended for precision parts
PTFE (teflon®)	2.1–2.2	0.48–0.76	260	$\approx 10^{-13}$	Produced by powder sintering; excellent self-lubricating properties; high chemical inertness
PTFE + glass or carbon fibers			260	$\approx 10^{-14}$	Reinforced to increase strength
Polyimide	1.42	2–3	320	$\approx 3 \times 10^{-15}$	Excellent mechanical properties (up to 250 °C). Quite expensive
Polyimide + graphite	1.5	5–14	320	$\approx 3 \times 10^{-16}$	Graphite reduces friction and wear
Phenolics	1.4	50	200	$\approx 10^{-14}$	
Phenolics + PTFE	1.4	50	200	$\approx 2 \times 10^{-16}$	

The specific wear rate, K_a, refers to dry sliding tests against steel; data obtained from various sources in the literature

thrust-bearing tester with a steel counterface [50]. For this material, the transition from mild to severe wear occurs when a surface critical temperature of 395 °C is reached. In the investigated tribological conditions, the limit value of the product between the applied pressure and sliding speed at which the contact temperature reaches 395 °C is 1 MPa m/s at 14 m/s, and 12 MPa m/s at 1.71 m/s. Table 6.9 lists some *maximum PV limits* (whose meaning is different to the PV_{limit} concept introduced in Sect. 5.1.4) for several polymeric materials dry sliding against a steel counterface and obtained using a similar testing geometry [50].

As said, polymeric composites containing particles or short fibres are commonly used in different applications. To reduce friction and wear (both determined by adhesion), lubricants such as PTFE and graphite flakes are typically employed,

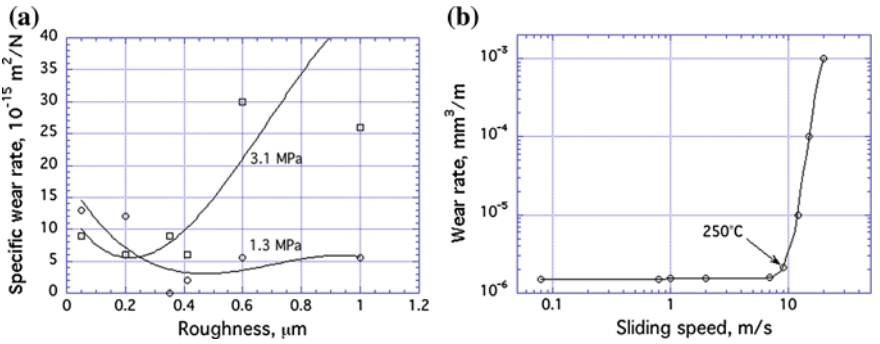

Fig. 6.23 Specific wear rate of Nylon 66: **a** role of the counterface roughness (counterface: 100Cr6, modified from [17]); **b** role of sliding velocity (steel counterface with R_a = 0.15 μm, modified from [49])

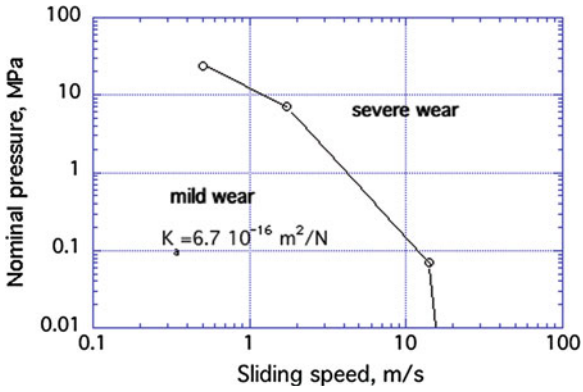

Fig. 6.24 Wear map for a polyimide containing 15 % of graphite dry sliding against steel (modified from [50])

whereas glass, carbon and aramid fibres are used to increase the mechanical strength and the Young's modulus. In some cases, both types of fillers are added together, to optimize the properties. For example, polyamide 66 (Nylon 66) composites containing both reinforcing and self-lubricating additions are often used. Typical compositions are: 20 % glass + 20 % PTFE; 30 % carbon + 15 % PTFE/silicon oil; 15 % aramid fibres + 10 % PTFE. As a further example, consider the polyimide composites listed in Table 6.9. The graphite containing composites display the best wear resistance (high PV limit), but they also display quite a high friction coefficient (around 0.31) during the run-in stage. With the addition of PTFE, the friction coefficient is 0.1 from the beginning of sliding. It should also be noted that polymers reinforced with hard fibres, such as glass fibres, could exert an abrasive action against the counterface material. Glass has a hardness of about 500 kg/mm^2 (Table 2.1) and the antagonists should therefore possess an hardness in excess of 700 kg/mm^2 in order to avoid abrasive wear. When using steels, they should be heat-treated or nitrided.

Table 6.9 Maximum PV limits for several polymeric materials (modified from [50])

Material	Maximum PV limit (MPa m/S)	Maximum contact temperature (°C)	Material	Maximum PV limit (MPa m/s)	Maximum contact temperature (°C)
PI-15 % graphite	12	395	PTFE	0.064	260
PI-40 % graphite	12	395	PTFE 15-25 % glass	0.45	260
PI-15 % graphite-10 %PTFE	3.6	260	PTFE-25 % carbon	0.71	260
Acetal	0.27	120	PTFE-60 % bronze	0.66	260
Acetal-PTFE	0.12	120	Nylon 66	0.14	150

A special mention has to be devoted to PTFE-based composites. Because of the high viscosity of PTFE even at high temperature, these materials are produced by mixing PTFE and fillers, pressing and sintering. Unreinforced PTFE is characterized by very high wear rates (Tables 6.8 and 6.9), but with proper additions wear resistance is greatly increased while maintaining the self-lubricating properties. It is supposed that fillers increase the load bearing capacity of the material and also favour the formation of a stable and compact transfer layer [51]. Recently it has been shown that the addition of low amounts of nano-fillers can decrease the PTFE wear by 4 orders of magnitude [52]. As an example, PTFE nanocomposites reinforced with α-alumina display an ultra-low steady state specific wear rate of around 10^{-16} m^2/N, after a run-in period necessary to form a high performing transfer layer [53].

A particular class of polymeric composites are the *organic friction materials*. They are used in automotive brake pads typically sliding against a grey pearlitic cast iron disc. These materials contain a thermosetting phenolic polymer (10–40 % in volume) that holds together a large amount of different additives [54]:

- Reinforcements, such as metal (steel, copper and bronze), carbon, glass and aramid fibres;
- Friction modifiers, such as graphite and metal sulphides particles that act as solid lubricants, and Al_2O_3, MgO and silica particles that act as abrasives;
- Fillers, such as vermiculite (a Mg silicate), barium sulphate and mica particles that improve the manufacturability and reduce cost.

At low loads and sliding speeds, dry sliding wear is mild. The specific wear rate of the organic friction materials is typically between 5×10^{-15} and 5×10^{-14} m^2/N. The friction coefficient is between 0.3 and 0.6, depending on the material composition. The so-called *low-metallic pads* contain a low amount of metal reinforcements and a high amount of abrasives and they are thus characterized by a

higher friction coefficient and also a higher wear than the so-called *NAO pads*, that constitutes an other important class of organic friction materials.

At high loads and sliding speeds, severe wear occurs. The transition takes place when a critical contact temperature in the range of 200–300 °C is attained [54]. At this temperature, the thermal degradation of the phenolic polymer occurs. This causes an increase in the wear rate, which then exponentially rises with contact temperature, and a decrease in the friction coefficient. Such a decrease has to be reduced to a minimum by carefully selecting the materials ingredients, in order to avoid jeopardizing the braking effectiveness. In applications where the attainment of quite high temperatures is usual (such as in train or aeroplane brakes), it is necessary to employ more resistant materials, such as sintered metals and carbon-carbon composites.

6.8.2 Abrasive Wear by Hard, Granular Material

Because of their low hardness, a very low abrasion resistance characterizes polymeric materials. In applications where a minimum abrasion resistance is required, it is appropriate to employ ultra-high molecular weight polyethylene (UHMW PE, a thermoplastic polymer) or elastomeric polyurethanes with high hardness.

Elastomers are a class of polymers with an adequate resistance to low-stress abrasion (at least in some applications). In particular, they display a good resistance to solid particle erosion wear in case of low impact velocity. This behaviour is mainly due to their low elastic moduli and high elastic limit, resulting in a high elastic deformation and rebound capability. Beside natural rubber, the elastomers that are mainly used are styrene butadiene rubber (SBR), for example in the production of automobile tires; chloroprene (CR), for example in the production of gaskets or conveyors; polyurethanes, for example in the production of idlers, cyclones and screens [27].

In case of relatively low impact velocities, elastomeric materials display Φ_{SPE}-values (representative of the efficiency of the process), in the range 10^{-3}–10^{-2} [55], and therefore similar, or lower, than those of steels. Table 6.10 shows the results of

Table 6.10 Normalized erosion rates for different engineering materials (data from [56])

Material	Hardness (kg/mm^2)	Relative erosion resistance
AISI 1018	254	1
Natural rubber	40 Shore A	14
Natural rubber	60 Shore A	3.6
Polyurethane	90 Shore A	1.1
35 % Cr 5 % C white iron	780	5.8
27 % Cr 3 % C white iron	621	3.1
Martensitic stainless steel	308	1.1
WC-3.3 % Co	2300	59

erosive tests carried out at low impact angles (lower than 10°), an impact velocity ranging from 14 to 24 m/s and using SiC erosive particles with high angularity [56]. The tests were conducted on two natural rubbers, a polyurethane and several materials for use in comparable applications. The results are expressed in terms of the relative erosion resistance (RER) by dividing the erosion rate of the reference AISI 1018 steel by that of the tested material. The results show that the natural rubbers, in particular the softer one, exhibit better erosion resistance than the polyurethane and also the martensitic stainless steel. The softest rubber also shows a better performance than the two cast irons under study. This behaviour was attributed by the Authors to the higher propensity of natural rubber to elastic recovery. As expected, the hard metal displays the best behaviour.

The applicability of elastomers in engineering applications is limited to a defined temperature range, between their T_g and their melting or decomposition temperature, which is typically in the range 80–130 °C.

References

1. W.A. Glaeser, *Materials for Tribology* (Elsevier, Amsterdam, 1992)
2. D.A. Rigney (ed.), *Fundamentals of Friction and Wear of Materials* (ASM, Metals Park, 1981)
3. M. Takeda, T. Onishi, S. Nakakubo, S. Fujimoto, Physical properties of iron-oxide scales on Si-containing steels at high temperature. Mater. Trans. **50**, 2242–2246 (2009)
4. H. Czichos, K.H. Habig, Wear of medium carbon-steel—a systematic study of the influences of materials and operating parameters. Wear **110**, 389–400 (1986)
5. S.C. Lim, M.F. Ashby, Wear-mechanism maps. Acta Metall. Mater. **35**, 1–24 (1987)
6. P. Clayton, Tribological aspects of wheel-rail contact: a review of recent experimental research. Wear **191**, 170–183 (1996)
7. H.K.D.H. Bhadeshia, Steels for bearings. Prog. Mater. Sci. **57**, 268–435 (2012)
8. A. Bhattacharyya, G. Subhash, N. Arakere, Evolution of subsurface plastic zone due to rolling contact fatigue of M-50 NiL case hardened bearing steel. Int. J. Fatigue **59**, 102–113 (2014)
9. I. Hucklenbroich, G. Stein, H. Chin, W. Trojhan, E. Streit, High nitrogen martensitic steel for critical components in aviation. Mater. Sci. Forum **318–320**, 161–166 (1999)
10. A.R. Lansdown, A.L. Price, *Materials to Resist Wear* (Pergamon Press, Oxford, 1986)
11. Z.Y. Yang, M.G.S. Naylor, D.A. Rigney, Sliding wear of 304 and 310 stainless steels. Wear **105**, 73–86 (1985)
12. K.H. Zum Gahr, *Microstructure and Wear of Materials* (Elsevier, Amsterdam, 1987)
13. N.S. Tiedje, Solidification, processing and properties of ductile cast iron. Mater. Sci. Technol. **26**, 505–514 (2010)
14. G. Straffelini, M. Pellizzari, L. Maines, Effect of sliding speed and contact pressure on the oxidative wear of austempered ductile iron. Wear **270**, 714–719 (2011)
15. G. Straffelini, L. Maines, The relationship between wear of semimetallic friction materials and pearlitic cast iron in dry sliding. Wear **307**, 75–80 (2014)
16. P.W. Leach, D.W. Borland, The unlubricated wear of flake graphite cast iron. Wear 85, 247–256 (1983)
17. K.H. Czichos, K.H. Habig, *Tribologie Handbuch*, *Reibung und Verlschleiss* (Vieweg, Wiesbaden, 1992)
18. N.A. Waterman, M.F. Ashby, *Elsevier Materials Selector* (Elsevier, Oxford, 1992)

19. R.C. Dommarco, J.D. Salvande, Contact fatigue resistance of austempered and partially chilled ductile irons. Wear **254**, 230–236 (2003)
20. V. Fontanari, M. Benedetti, G. Straffelini, Ch. Girardi, L. Giordanino, Tribological behavior of the bronze-steel pair for worm gearing. Wear **302**, 1520–1527 (2013)
21. G. Straffelini, L. Maines, M. Pellizzari, P. Scardi, Dry sliding wear of Cu-Be alloys. Wear **259**, 506–511 (2005)
22. C.T. Kwork, P.K. Wong, H.C. Man, F.T. Cheng, Sliding wear and corrosion resistance of copper-based overhead catenary for traction systems. IJR Int. J. Railway **3**, 19–27 (2010)
23. M.M. Khonsari, E.R. Booser, *Applied Tribology*, 2nd edn. (Wiley, West Sussex, 2008)
24. M.J. Neale, M. Gee, *Guide to Wear Problems and Testing for Industry* (Professional Engineering Publishing, London, 2000)
25. W.M. Rainforth, A.J. Leonard, C. Perrin, A. Bedolla-Jacuinde, Y. Wang, H. Jones, Q. Luo, High resolution observations of friction-induced oxide and its interaction with the worn surface. Tribol. Int. **35**, 731–748 (2002)
26. G. Straffelini, A. Molinari, Mild sliding wear of Fe-0.2 % C, Ti-6 % Al-4 % C and Al-7072: a comparative study. Tribol. Lett. **41**, 227–238 (2011)
27. K.G. Budinski, M.K. Budinski, *Engineering Materials*, *Properties and Selection* (Prentice Hall, Upper Saddle River, 2002)
28. S. Wilson, A.T. Alpas, Wear mechanism maps for metal matrix composites. Wear **212**, 41–49 (1997)
29. A. Molinari, G. Straffelini, B. Tesi, T. Bacci, Dry sliding wear mechanisms of the Ti6Al4 Va alloy. Wear **208**, 105–112 (1997)
30. A. Molinari, G. Straffelini, B. Tesi, T. Bacci, G. Pradelli, Effects of load and sliding speed on the tribological behaviour of Ti-6Al-4V plasma nitrided at different temperatures. Wear **203–204**, 447–454 (1997)
31. R. Bailey, Y. Sun, Unlubricated sliding friction and wear characteristics of thermally oxidized commercially pure titanium. Wear **308**, 61–70 (2013)
32. G. Straffelini, A. Andriani, B. Tesi, A. Molinari, E. Galvanetto, Lubricated rolling-sliding behaviour of ion nitrided an untreated Ti-6Al-4V. Wear **256**, 346–352 (2004)
33. B. Bushan, *Introduction to Tribology* (Wiley, New York, 2002)
34. H.S. Kong, M.F. Ashby, Wear mechanisms in brittle solids. Acta Metall. Mater. **40**, 2907–2920 (1992)
35. S.M. Hsu, M. Shen, Wear prediction of ceramics. Wear **256**, 867–878 (2004)
36. K. Adachi, K. Kato, N. Chen, Wear map of ceramics. Wear **203–204**, 291–301 (1997)
37. K. Kato, Wear in relation to friction—a review. Wear **241**, 151–157 (2000)
38. J. Takadoum, *Materials and Surface Engineering in Tribology* (Wiley, London, 2008)
39. J. Xu, K. Kato, Formation of tribochemical layer of ceramics sliding in water and its role for low friction. Wear **245**, 61–75 (2000)
40. B. Bushan (ed.), *Modern Tribology Handbook*, vol. 2 (CRC Press, Boca Raton, 2001)
41. J.G. Chacon-Nava, F.H. Stott, S.D. de la Torre, A. Martinez-Villafane, Erosion of alumina and silicon carbide at low-impact velocities. Mater. Lett. **55**, 269–273 (2002)
42. A.F. Colclough, J.A. Yeomans, Hard particle erosion carbide and silicon carbide-titanium diboride from room temperature to 1000 °C. Wear **209**, 229–236 (1997)
43. I.M. Hutchings, *Tribology* (Edward Arnold, London, 1992)
44. J. Pirso, S. Letunovits, M. Voljus, Friction and wear behaviour of cemented carbides. Wear **257**, 257–265 (1997)
45. J. Pirso, M. Voljus, K. Juhani, S. Letunovits, Two-body dry abrasive wear of cermets. Wear **266**, 21–29 (2009)
46. B. Vankataraman, G. Sundararajan, The influence of sample geometry on the friction behaviour of carbon-carbon composites. Acta Metall. Mater. **50**, 1153–1163 (2002)
47. F. Cardarelli, *Materials Handbook*, 2nd edn. (Springer, New.York, 2008)
48. G. Straffelini, P. Scardi, A. Molinari, R. Polini, Characterization and sliding behaviour of HF CVD diamond coatings on WC-Co. Wear **249**, 461–472 (2001)

49. D.C. Evans, J.K. Lancaster, *Wear*, *Treatise on Materials Science and Technology* (Academic Press, London, 1979)
50. Vespel line Design Handbook, Du Pont. http://dupont.com/vespel
51. J. Khedkar, I. Negulescu, E. Meletis, Sliding wear behavior of PTFE composites. Wear **252**, 361–369 (2002)
52. K. Friedrich, Z. Zhang, A.K. Schlarb, Effects of various fillers on the sliding wear of polymer composites. Compos. Sci. Technol. **65**, 2329–2343 (2005)
53. J. He, H.S. Khare, D.L. Burris, Quantitative characterization of solid lubricant transfer film quality. Wear **316**, 133–143 (2014)
54. A.E. Anderson, Friction and wear of automotive brakes. ASM Handb. **18**, 569–577 (1992)
55. S. Arjula, A.P. Harsha, Study of erosion efficiency of polymers and polymer composites. Polym. Test. **25**, 188–196 (2006)
56. L.C. Jones, Low angle scouring erosion behaviour of elastomeric materials. Wear **271**, 1411–1417 (2011)